



# STUDY OF EMISSION OF LIGHT FROM NANOPOROUS SILICON QUANTUM DOT

By Adem Beriso

SUBMITTED IN PARTIAL FULFILLMENT OF THE  
REQUIREMENTS FOR THE DEGREE OF  
MASTER OF SCIENCE IN PHYSICS

AT

ADDIS ABABA UNIVERSITY  
ADDIS ABABA, ETHIOPIA

June, 2010

© By Adem Beriso, 2010



ADDIS ABABA UNIVERSITY  
DEPARTMENT OF  
PHYSICS

The undersigned hereby certify that they have read and recommend to the Faculty of Science, school of Graduate Studies for acceptance a thesis entitled “**STUDY OF EMISSION OF LIGHT FROM NANOPOROUS SILICON QUANTUM DOT**” by Adem Beriso in partial fulfillment of the requirements for the degree of Master of Science in physics.

Dated: June, 2010

Name	Signature
Dr. S. K. Ghoshal, Advisor	_____
Dr. Tesgera Bedassa, Examiner	_____
Professor Malnev, Examiner	_____

ADDIS ABABA UNIVERSITY  
DEPARTMENT OF  
PHYSICS

Date: **June, 2010**

Author: **Adem Beriso**

Title: **STUDY OF EMISSION OF LIGHT FROM NANOPOROUS SILICON  
QUANTUM DOT**

Department: **Physics**

Degree: **M.Sc.**

Convocation: **June**

Year: **2010**

Permission is herewith granted to Addis Ababa University to circulate and to have copied for non-commercial purposes, at its discretion, the above title upon the request of individuals or institutions.

Signature of Author.....

THE AUTHOR RESERVES OTHER PUBLICATION RIGHTS, AND NEITHER THE THESIS NOR EXTENSIVE EXTRACTS FROM IT MAY BE PRINTED OR OTHERWISE REPRODUCED WITHOUT THE AUTHOR'S WRITTEN PERMISSION.

THE AUTHOR ATTESTS THAT PERMISSION HAS BEEN OBTAINED FOR THE USE OF ANY COPYRIGHTED MATERIAL APPEARING IN THIS THESIS (OTHER THAN BRIEF EXCERPTS REQUIRING ONLY PROPER ACKNOWLEDGEMENT IN SCHOLARLY WRITING) AND THAT ALL SUCH USE IS CLEARLY ACKNOWLEDGED.

For the remembrance of my mother **Tayibe Badhane** and my  
father **Beriso Bejo**

# Table of Contents

Table of Contents	v
List of Figures	vii
Abstract	x
Acknowledgments	xi
<b>Chapter One: Introduction</b>	<b>1</b>
1.1 What are nano-structures? .....	1
1.2 Quantum confinement effect on the size of nanostructure .....	2
1.2.1 Density of states in view of quantum confinement .....	3
1.3 Preparation of porous silicon .....	5
1.4 Energy gap of nanostructures .....	8
1.5 The k.p perturbation theory.....	9
1.6 Applications of Si nanostructure.....	11
1.7 Porous Silicon and Its Properties .....	12
1.7.1 Electronic Properties .....	13
1.7.2 Electrical Properties .....	13
1.7.3 Light emitting properties.....	14
1.8 objectives.....	16
1.8.1 General objective.....	16
1.8.2 Specific objective.....	16
1.9 Thesis outline.....	16

<b>Chapter Two: Photoluminescence</b>	<b>17</b>
2.1 Introduction .....	17
2.2 Mechanism of visible light emission from nanoporous silicon .....	18
2.3 Examples of photoluminescence materials .....	19
2.4 Importance of photoluminescence materials .....	20
<b>Chapter Three: Optical behavior of nanoporous silicon quantum dot</b>	<b>21</b>
3.1 Optical parameters .....	21
3.1.1 Absorption coefficients.....	21
3.1.2 Dielectric function.....	23
3.1.3 Oscillator strength .....	25
3.2 Effect of temperature on the optical properties of porous silicon .....	26
3.3 Effect of surface states on photoluminescence .....	27
3.4 Formation of a model to generate photoluminescence spectra.....	30
<b>Chapter Four: Model, Results and Discussions</b>	<b>34</b>
4.1 Dependence of optical energy gap on porosity parameters $c$ and $\alpha$ of nanoporous silicon quantum dot.....	36
4.2 Dependence of optical absorption coefficient on porosity level of nanoporous silicon quantum dot .....	38
4.3 Dependence of imaginary part of the dielectric function on porosity level of nanoporous silicon quantum dot.....	41
4.4 Dependence of Oscillator strength on porosity level of nanoporous silicon quantum dot.....	43
4.5 Factors that affect peak of photoluminescence .....	45
<b>Chapter Five: conclusions and future outlook</b>	<b>49</b>
<b>Appendices</b>	<b>51</b>
<b>Bibliography</b>	<b>56</b>

# List of Figures

1.1. Bulk Si (left) and Si nanostructure (right) [3] .....	2
1.2. The density of states as a function of energy for a particle confined to move in a bulk, quantum well, quantum wire and quantum dot . As can be seen from the above diagrams the density of states varies as a function of energy from atomic to bulk regime. It logically follows that optical and electronic properties drastically change as one goes from bulk to atomic level (nano-scale),which mainly evolves from quantum-confinement effect[7].....	5
1.3. The use of bottom-up and top-down techniques in manufacturing [9].....	6
1.4. Formation of porous silicon. (Left) SEM image illustrating the three typical etching regimes in silicon: porous formation, transition regime with pillar-like structures, and electropolishing [10]. (Right) TEM micrograph of porous silicon grains with characteristic size of several nanometers [11].....	7
1.5. Size quantization effect. Electronic state transition from bulk to small cluster [15].....	8
1.6. Calculated optical gap energies for Si-crystals depending on their diameter [9, 10].....	13
1.7.a) I – V characteristic for oxidized P-Si samples at Room Temperature (RT); b) I – T characteristic for Oxidized P-Si samples.....	14
1.8. AFM image (656×656 nm) of light-emitting porous silicon [30]. . . . .	15
2.1. Photoluminescence. On the left a high energy laser photon gets out an electron from its orbit. The electron loses energy until it reaches the bottom of the conduction band. The right hand diagram shows two possible transitions. On the left the electron combines immediately with a hole in the valence band emitting a photon of energy $E_g$ . On the right it gets stuck in a 'between-gap' state emitting a lower energy photon [34].....	19

3.1. A schematic energy diagram for atoms and molecules, and also the bulk and the surface of a silicon crystal [27]. .....	28
3.2. Room temperature photoluminescence spectra from porous silicon samples with different porosities kept under Ar atmosphere (a) and after exposure to air (b) [27].....	29
3.3. Silicon nanocrystals embedded in SiO <sub>2</sub> [29]. .....	30
4.1. Variation of optical energy gap with porous silicon nanocluster (quantum dot) diameter. The upper line (blue) is for $\alpha = 1.32$ (10% to 20% porosity) and the lower line (green) is for $\alpha = 1.42$ (30% to 40% porosity). For both lines $c = 4.5$ .....	37
4.2. Variation of optical energy gap with porous silicon nanocluster (quantum dot) diameter. The upper line (blue) is for $\alpha = 1.32$ (10% to 20% porosity) and the lower line (green) is for $\alpha = 1.42$ (30% to 40% porosity). For both lines $c = 6.2$ . .....	38
4.3. Optical absorption coefficient as a function of porous silicon nanocluster (quantum dot) size at a give photon energy $\hbar\omega = 3\text{eV}$ . For both pure and passivated samples $\alpha = 1.32$ (10% to 20% porosity). .....	39
4.4. Optical absorption coefficient as a function of porous silicon nanocluster (quantum dot) size at a given photon energy $\hbar\omega = 3\text{eV}$ . For both pure and passivated samples $\alpha = 1.42$ (30% to 40% porosity).....	40
4.5. Imaginary part of dielectric function as a function of porous silicon nanocluster (quantum dot) size at a given photon energy $\hbar\omega = 3\text{eV}$ . For both pure and passivated samples $\alpha = 1.32$ (10% to 20% porosity).....	42
4.6. Imaginary part of dielectric function as a function of porous silicon nanocluster (quantum dot) size at a given photon energy $\hbar\omega = 3\text{eV}$ . For both pure and passivated samples $\alpha = 1.42$ (30% to 40% porosity). .....	43
4.7 Oscillator strength as a function of porous silicon nanocluster (quantum dot) size at a given photon energy $\hbar\omega = 3\text{eV}$ . For both pure and passivated samples $\alpha = 1.32$ (10% to 20%	

porosity).....	44
4.8. Oscillator strength as a function of porous silicon nanocluster (quantum dot) size at a given photon energy $\hbar\omega=3\text{eV}$ . For both pure and passivated samples $\alpha = 1.42$ (30% to 40% porosity).....	45
4.9. Normalized PL intensity versus size of nanoporous silicon cluster (quantum dot) for $\gamma = 1.32$ (10% to 20% porosity).....	46
4.10. Normalized PL intensity versus size of nanoporous silicon cluster (quantum dot) for $\gamma = 1.42$ (30% to 40% porosity). . . . .	47
4.11. Normalized PL intensity versus size of nanoporous silicon cluster (quantum dot) for $\gamma = 1.32$ (10% to 20% porosity). . . . .	48

# Abstract

Both nanocrystalline and nanoporous silicon shows interesting optical and light emission properties. As the system size goes to nanoscale the optical band gap, radiative transitions, oscillator strength, absorption coefficient and dielectric function increases. The nanosilicon shows unusual optical properties which have tremendous importance for nanophotonics and optoelectronic applications. The purpose of the thesis is to study the light emission and optical behavior of nanoporous silicon cluster (quantum dot) with varying porosity and oxygen as well as hydrogen at the surface. We examine these properties combining k.p perturbation method and surface state model. In order to clarify the morphological effects such as size, surface passivation and porosity level of a nanoporous silicon cluster on its optical properties, calculation of optical absorption coefficient, dielectric function and oscillator strength of porous silicon nanoclusters as a function of size (diameter) through energy gap is discussed using k.p method. The effects of nanoparticles size along with surface passivation and porosity level on optical band gap have also been investigated and compared with experiment. The porosity and surface effects are incorporated through some empirical parameters  $c$  and  $\alpha$  in our model. Furthermore, we examine the main factors that causes photoluminescence peak to shift towards left or to the smaller wavelength of visible spectrum (blue shifted). Our results are in conformity with some other experimental and theoretical findings. We also present some of the important applications of silicon nanostructures and provide a control mechanism for light emission through our investigation.

# Chapter One

## Introduction

Recently, there has been a substantial amount of interest in Si nano-structures. This is due to the observation of visible photoluminescence (PL) in these materials, which promised potential applications in optoelectronic devices [1].

Since the early 60's silicon has been the dominating material of microelectronics because of its excellent mechanical, chemical and electrical properties. The report by Canham, Lehmann and Gisele about the visible and efficient photoluminescence from porous silicon attracted a large attention of researchers which resulted in more than 1500 paper published since 1990. Light emitting silicon nanostructures have since been produced by using a wide range of different techniques. Initial excitement surrounded porous silicon (por-Si) because it represents an inexpensive and easily prepared form of nanostructure silicon. Quantum confinement effects are prominent in por-Si which has led to a wide range of studies into its optoelectronic properties. While an explanation of Canham's observation of visible light emission has motivated most of the work on por-Si, increasingly interest has developed in por-Si as a bio-compatible material and as a component of chemical and biochemical sensors. In this chapter we are going to discuss what nano-structures are, quantum confinement effect on this nano-structures, formation of porous silicon, K.P perturbation theory and properties of Porous Silicon.

### 1.1 What are nano-structures?

The prefix 'nano' is derived from the Greek word for dwarf. But "Nano" now refers to dimensions that are one billionth times smaller than a meter or simply  $10^{-9}$ m. Structures of materials characterized by dimensions in the order of nanometer constitute nano-structures. Nano-structures are seen as the key for many applications in data storage and communication technology. A nano-meter is incredibly small, about 50,000 times finer than human hair and still 200 times smaller than

the finest lithographic feature in micro-chips. In this size regime, the law of quantum mechanics predominates. These nano-structures are of huge technological interest since many of their optical and electronic properties show strong size dependence. The inherent size dependence of macroscopic nano-crystal properties is the result of two primary mechanisms, free energy variation and quantum confinement. Nano-crystals have the ability to have their free energy manipulated in a controlled manner, correlated with particle size. Generally reducing any piece of material from a chunk to a nanometer scale changes virtually all of its basic properties in a fundamental way. Its shape and crystalline structure change, as do its melting and boiling temperatures. Material properties change dramatically because quantum effects arise from the confinement of electrons and holes in the materials [2]. The quantum confinement effect is one of the factors that alter the basic properties of the material which we will see in the next section.

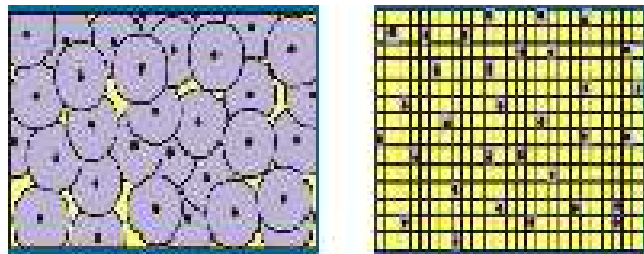


Figure .1.1. Bulk Si (left) and Si nanostructure (right) [3].

## 1.2 Quantum confinement effect on the size of nanostructures

Semiconductor nano-crystals having analogous interior bonding geometries compared to their known bulk counterparts exhibit variations in their optical properties with size variation. The main concern for these changes lies in the variation of density of states as a function of energy, which varies as a function of dimension of nanostructures. From a density of state perspective nano-crystals lie between discrete atomic and bulk limit. In any material there will be a size below which one observes fundamental electronic and optical properties as a function of size. This quantum size effect regime begins when the

energy level spacing exceeds  $k_B T$  (energy level spacing  $> k_B T$ ). If we confine the electron-hole pairs (excitons) in a small region, having dimensions of the order of a few nano-meters, the properties of the material completely change. Since the order of magnitude of the electron and hole De-Broglie's wavelength ( $\sim 1\text{nm}$ ) is comparable with the confinement dimensions, they behave as particles in a box. Consequently, the confinement effect in a region of nano-metric size is referred to as quantum confinement and it has an effect in widening the band-gap of nano-structures.

One of the most direct effects of reducing the size of materials to the nanometer range is the appearance of quantization effects due to the confinement of the movement of electrons, this leads to discrete energy levels depending on the size of the structure. Following this line artificial or natural structure with properties different from the corresponding bulk materials can be created. Control over dimensions as well as composition of structures makes it possible to tailor material properties to specific applications which are influenced by quantum confinement effect (QCE) [4]. Hence, Quantum confinement (QC) in semiconductors results from the geometric confinement of electrons, holes or excitons (electron hole bound pair). The normal size of an exciton in a large bulk crystal is expressed as an exciton Bohr radius (BER). When an electron-hole pair is squeezed below the dimensions approaching exciton Bohr radius, quantum confinement effects become prominent in the structure and the effective band gap increases. The smaller the nanostructure the larger the effective band gap and the greater the energy of optical emission which changes the optical and electronic properties when the sample size is sufficiently smaller than 10 nm. This effect can also be understood from Heisenberg's uncertainty principle according to which energies of an electron or hole increase as their position is confined. As a result the effect of QC is a rearrangement of the density of electronic states in energy as direct consequence of volume shrinking in one, two, or even three dimensions, which can be obtained, respectively, in quantum wells, wires, and dots. Thus understanding of the spatial confinement of electrons within the crystallite boundary leads to a larger spacing between band gap to change various properties and physical structure of the material as the size of the nanostructure decreased [5].

### **1.2.1 Density of states in view of quantum confinement**

As a result of quantum confinement in different directions, there is a change in wave function describing the behaviour of electrons and holes and consequently the number of states per unit energy, i.e. the density of states changes as a function of energy  $E$  of the particle. Generally the density of states

depends on the dimension of the nano-structure and the corresponding wave vector dispersion [6]. In case of a bulk-material, the density of states increases with energy of the particle following a parabolic law. Therefore for a three dimensional bulk material, the DOS is defined as the number of available electronic states per unit volume per unit energy E and it is given by:

$$D(E) = \frac{\sqrt{2}m_e^{\frac{3}{2}}}{\pi^2\hbar^3} E^{\frac{1}{2}} \quad (1.2.1)$$

Where as in the case of two-dimensional nano-structures (quantum well) the carrier movement is restricted to a plane (the two directions are for the movement of particles, while the third direction determines the quantum confinement direction). The DOS is defined as the number of electronic states per unit area per unit energy and it is given by:

$$D(E) = \frac{m_e}{\pi^2\hbar^2} \quad (1.2.2)$$

Further reduction in the dimension of a system ends up in a quantum-wire. Examples of such one-dimensional structures include nano-tubes, semiconductor nano-wires and nano-rods. For a quantum wire (particles are free to move in only one direction and the two sides are confined) the DOS is defined as the availability of electronic states per unit length per unit energy and is given by:

$$D(E) = \frac{\sqrt{2}m_e^{\frac{1}{2}}}{\pi\hbar} E^{-\frac{1}{2}} \quad (1.2.3)$$

Finally for a zero dimensional system (quantum dot), the confinement is along all three dimensions and the DOS becomes a delta function. In the 0-D (strong confinement) the electrons are confined in their motion in all three directions [7].

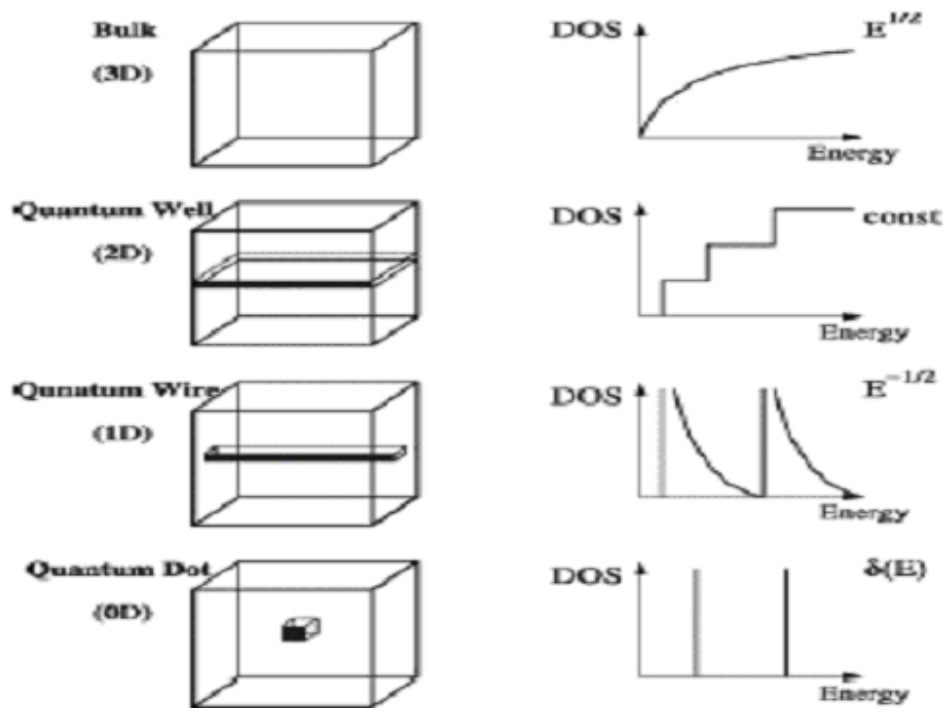


Figure .1.2. The density of states as a function of energy for a particle confined to move in a bulk, quantum well, quantum wire and quantum dot. As can be seen from the above diagrams the density of states varies as a function of energy from atomic to bulk regime. It logically follows that optical and electronic properties drastically change as one goes from bulk to atomic level (nano-scale), which mainly evolves from quantum-confinement effect [7].

### 1.3 Preparation of porous silicon

Generally there are a wide variety of techniques that are capable of creating nanostructures with various degrees of quality, speed and cost. These manufacturing approaches fall under two categories: ‘bottom-up’, and ‘top-down’. In recent years the limits of each approach, in terms of feature size and quality that can be achieved, have started to converge. A diagram illustrating some of the types of materials and products that these two approaches are used for is shown below in Figure .1.3. In this thesis we are going to see formation of nanoporous silicon only.

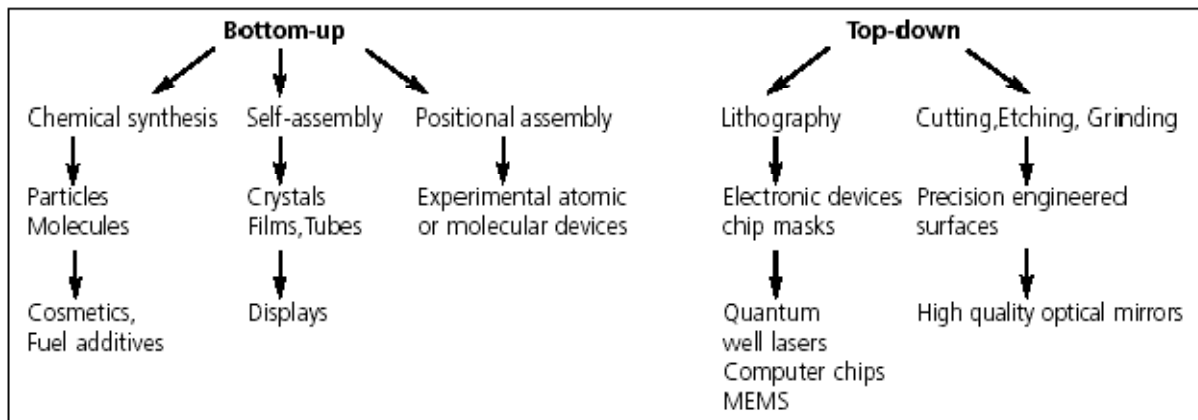


Figure.1.3. The use of bottom-up and top-down techniques in manufacturing [9]

Porous silicon (PS) with its distribution of size is a highly disordered material, i.e., porous silicon is a disordered system. The disorder plays a key role and models it by a distribution of crystallite sizes. Porous silicon (PS), whose structural investigations have confirmed that it consists of silicon nanocrystals assemblies of different size (typically a few nm) and shape, is formed by electrochemical anodization of bulk silicon in an HF electrolyte [Fig.(1.4)]. The solution employed is typically aqueous 50 percent HF mixed with ethanol. The electrical source chosen for the process is usually current controlled, because the current density and the porosity are directly related. The anodization reaction at the Si/electrolyte interface requires the presence of holes [8]. Therefore, the natural choice for substrate doping is p-type. However, n-type substrates can also be employed for porous silicon fabrication, provided that generation mechanisms for excess holes are available- for example, by using light beam, or by biasing the substrate in the breakdown regime.

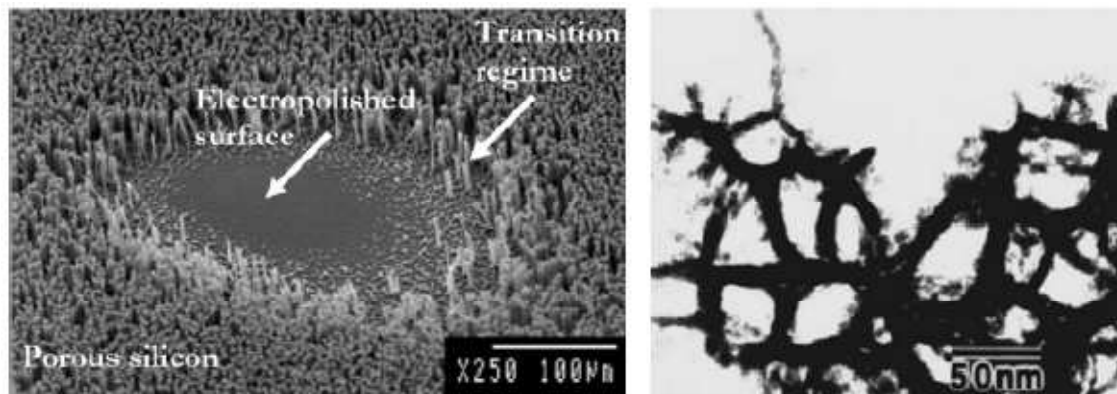


Figure.1.4. Formation of porous silicon. (Left) SEM image illustrating the three typical etching regimes in silicon: porous formation, transition regime with pillar-like structures, and electropolishing [10]. (Right) TEM micrograph of porous silicon grains with characteristic size of several nanometers [11].

Depending on the type of doping (p- or n-types) and the doping level of the wafer the sizes of pores and remaining silicon crystallites can be varied from micrometers to nanometers. Porous silicon fabricated on lightly p-type-doped substrates has an average nanocrystal size of 2-5 nm. Since the exciton Bohr radius of silicon is around 4.3nm, quantum confinement effects and in particular, large values of photoluminescence (PL) efficiency are especially evident in this type of porous silicon.

On the other hand, in highly p-type-doped wafer (i.e. with typical resistivity values around  $0.01\Omega$  cm), the size of the pores and structures is of the order of 10 nm. The quantum confinement effects are in this case less important, thus explaining why the Photoluminescence emission is remarkably weaker in low-resistivity porous silicon. However, carrier transport can be turned over a much wider range, and larger porosity ranges can be obtained. This preparation procedure has attracted much interest due to its simplicity, different from costly litho-graphic or epitaxial techniques that were at the time the conventional approaches to realize nanosized semiconductor [8].

Porous layer is a complicated network of silicon wires each with a thickness of between 2-5 nm (20,000 times thinner than a human hair). The porosity of a sample is defined as the amount of air in the material after processing has finished, so a 45 percent porous sample would contain 45 percent air and 55 percent silicon. A typical sample could have an internal surface area of up to several hundred square meters

per cubic centimeter. The strong deterioration of the mechanical properties with increasing porosity and its electroluminescence degradation during operation can be avoided by subsequently oxidizing the porous silicon layer using electrochemical anodization.

### 1.4 Energy gap of nanostructures

The size quantization effect that has been looked into at great lengths only recently leads to an important change in various properties such as electrical property, optical transitions, conductivity, magnetization, etc, start to change. These different behaviors of most materials reflect the different character of the band gap i.e. the difference in energy between the lowest point of empty conduction band and the highest fulfilled point of the valence band [14]. Therefore downscaling of purely classical bulk material properties can lead to dramatic changes in behavior in the nanoscale. Nevertheless the most exciting effects in the nanorealm where quantum physics comes into play and leads to completely new kinds of behavior causes the band gap ( $E_g$ ) to expand which means size quantization effect increases the energetic gap between the highest occupied and lowest unoccupied molecular orbitals (HOMO-LUMO gap), shifting the band gap from 1.12 eV in bulk Si all the way in to nanoclusters as shown below [15].

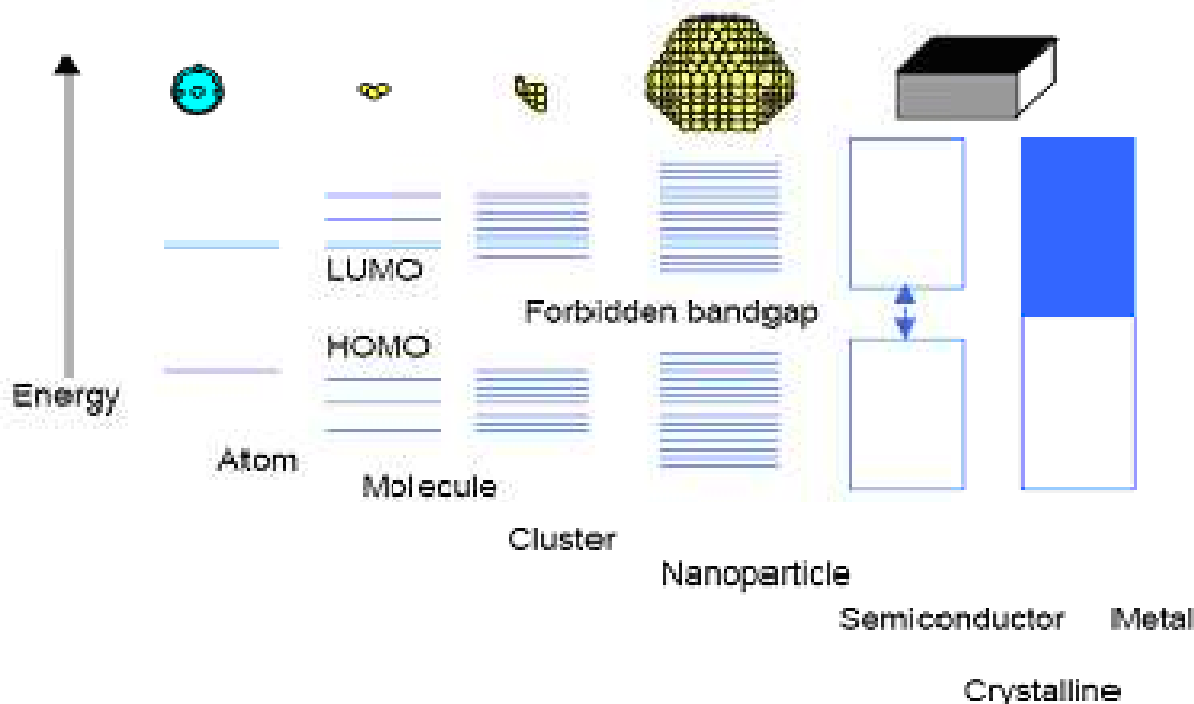


Figure. 1.5. Size quantization effect. Electronic state transition from bulk to small cluster [15].

## 1.5 The k.p perturbation theory

The K.P perturbation theory is used to explore the band structure at  $k = 0$  or other points  $k \neq 0$  of the Brillouin zone boundaries. This theory is based on a perturbation approach  $\hbar \vec{k} \cdot \frac{\mathbf{P}}{m}$  term in the Hamiltonian, applied to the Bloch wave functions  $\psi(\mathbf{K}, \mathbf{r})$ . The wave function is given by:

$$\psi = U_n(\mathbf{k}, \mathbf{r}) \exp(i\mathbf{k} \cdot \mathbf{r}) = \left[ \sum_l c_n U_{l0}(\mathbf{r}) \right] \exp(i\mathbf{k} \cdot \mathbf{r}) \quad (1.5.1)$$

Introducing this wave function in to one-electron Schrodinger equation one obtains:

$$\left( \frac{-\hbar^2}{2m_0} \nabla^2 + v(\mathbf{r}) + \frac{\hbar}{m_0} \mathbf{K} \cdot \mathbf{P} + \frac{\hbar^2 k^2}{2m_0} \right) U_n(\mathbf{K}, \mathbf{r}) = E_n(\mathbf{k}) U_n(\mathbf{K}, \mathbf{r}) \quad (1.5.2)$$

The first two terms in the Hamiltonian define the unperturbed Hamiltonian  $H_0$ , and the last two terms are due to small perturbations at a given  $\mathbf{K} \neq \mathbf{K}_0$ . Hence equation (1.5.2) can be expressed as:

$$\left[ H_0 + \frac{\hbar}{m_0} (\mathbf{K} - \mathbf{K}_0) \cdot \mathbf{P} + \frac{\hbar^2}{2m_0} (\mathbf{k} - \mathbf{k}_0)^2 \right] U_n(\mathbf{K}, \mathbf{r}) = E_n(\mathbf{K}) U_n(\mathbf{K}, \mathbf{r}) \quad (1.5.3)$$

However the Schrodinger equation for the unperturbed Hamiltonian can be re-written as:

$$H_0 U_{l0}(\mathbf{r}) = E_l(0) U_{l0}(\mathbf{r}) \quad (1.5.4)$$

when we insert equation (1.5.1) in to equation (1.5.3) and use equation 1.5.4, we obtain:

$$\sum c_l \left[ E_l(0) + \frac{\hbar}{m_0} (\mathbf{k} - \mathbf{k}_0) \cdot \mathbf{p} + \frac{\hbar^2}{2m_0} (\mathbf{k} - \mathbf{k}_0)^2 \right] U_{l0}(\mathbf{r}) = \sum c_l E_l(\mathbf{k}) U_l(\mathbf{r}) \quad (1.5.5)$$

Now multiplying equation (1.5.5) by  $U_{m_0}^*(r)$  and integrating over a unit cell  $v_c$  to obtain:

$$c_m[E_n(\mathbf{K}) - E_m(0) - \frac{\hbar^2 k^2}{2m_0}] - \sum_l c_l \frac{\hbar}{m_0} (\mathbf{K} \cdot M_{lm}) = 0 \quad (1.5.6)$$

When we write the above equation in matrix form, the numbers of  $\mathbf{K}$ .p matrix elements are greatly reduced because of symmetry considerations. These matrix elements are expressed as:

$$M_{lm}(\mathbf{K}_0) = \int \psi_{l0}^*(K, r) P \psi_{m0}(K, r) dr \quad (1.5.7)$$

Therefore the Eigen functions near a characteristic point  $\mathbf{K}_0$  can be expressed as:

$$E_n(\mathbf{K}) = E_n(\mathbf{K}_0) + \frac{\hbar^2}{2m_0} (\mathbf{K} - \mathbf{K}_0)^2 + \frac{\hbar^2}{m_0^2} \sum_{m \neq n} \frac{(\mathbf{K} - \mathbf{K}_0) \cdot M_{mn}(\mathbf{K}_0)}{E_n(\mathbf{K}_0) - E_m(\mathbf{K}_0)} \quad (1.5.8)$$

Equation (1.5.7) can be simplified when interactions between two bands are of interest (e.g. the valance and conduction bands). The reason why we take these two bands is due to the fact that the energy difference between these two bands is small compared to the difference with all other bands. Then we can write:

$$E_n(\mathbf{K}) = E_n(\mathbf{K}_0) + \frac{\hbar^2}{2} \sum \frac{(K_x - K_0)^2}{m_i^*} + \frac{(K_y - K_0)^2}{m_i^*} + \frac{(K_z - K_0)^2}{m_i^*} \quad (1.5.9)$$

Where  $m_i^*$  is the effective mass which can be expressed as:

$$\frac{1}{m_i^*} = \frac{1}{m_0} \pm \frac{2|M_{mn}(K_0)|^2}{m_0^2(E_m(K_0) - E_n(K_0))} \quad (1.5.10)$$

With the +ve for the conduction band and -ve for the valance band. We can use equation (1.5.9) for the deviation of  $E(\mathbf{K})$  from parabolicity near a critical point  $\mathbf{K}_0$

$$E(\mathbf{K}-\mathbf{K}_0) = \frac{-E_g}{2} + \frac{\hbar^2(K-K_0)^2}{2m_o} \pm \frac{1}{2} \sqrt{(E_g)^2 + \frac{4\hbar^2(K-K_0)^2 |M_{m_o}(K_0)|^2}{m_o^2}} \quad (1.5.11)$$

This gives with equation (2.3.10)

$$E(\mathbf{K} - \mathbf{K}_0) = \frac{-E_g}{2} + \frac{\hbar^2(K-K_0)^2}{2m_o} \pm \frac{-E_g}{2} \sqrt{1 + \frac{2\hbar^2(K-K_0)^2}{E_g} \left(\frac{1}{m^*} - \frac{1}{m_o}\right)} \quad (1.5.12)$$

Where  $m^*$  is the effective mass in the conduction (+) and valance (-) bands. This calculation illustrates how the K.P method is useful in predicting the band-structure of a nano-cluster at zone boundaries. The quantum confinement effect is responsible for the increment of the band-gap of nano-clusters. In addition to quantum confinement the size, shape and passivation of hydrogen and oxygen samples affects the band-gap of nano-size particles (nano-dots). According to many calculations and observations:

$$E_g^{nano} = E_g^{bulk} + \frac{c}{d^\alpha} \quad (1.5.13)$$

Where  $c$  is a constant and  $\alpha$  ranges from 1.25 to 1.85 and depends on the type of passivation as well as the symmetry of nanoclusters (the values of  $c$  and  $\alpha$  depend on the nature of the surface as well as the symmetry of nanoclusters). The main concern of this section was to find out the analytic calculations for the band energies using the K.P perturbation method.

## 1.6 Applications of Si nanostructure

Low-dimensional semiconductor structures are of high interest due to the significant technological implications in optics and nanoelectronics. The wide interest in nanosolid or porous silicon (P-Si) resulted primarily from the proposal, in 1990, that efficient visible light emission from high porosity structures. However, nanoscale silicon is a complex material with regard to its stability, because its optical properties

show environmental and ageing degradation with resulting ambiguity in device performance evaluation. Silicon nanostructures have tremendous applications in optoelectronic, emission of light and photonic devices. They can be easily integrated into silicon wafer processing and utilized for biological and chemical sensing, potential applications in silicon-based optoelectronic integrated circuits or for light-emitting devices, optical sensors, photo sensors, catalysts and memory devices. Silicon nanostructures can be used for optical communication technology to develop photonic integrated circuits: optical chips in which optical signals are guided, split, switched, multiplexed or amplified [4].

## **1.7 Porous Silicon and Its Properties**

Ever since the discovery of photoluminescence in an indirect bandgap materials like Si upon electrochemically etching a Si wafer as reported by Leigh Canham in 1990, there has been a tremendous interest in the study of these electrochemically etched crystalline Si materials, called porous Silicon (P-Si). It is sponge like structure with features (i.e. pores and undulating wires) with size of the order of few nm and has interesting characteristics such as larger surface area to volume ratio, highly nanoporous structure (controllable property), versatile, unstable due to porosity, which suggest other potential applications besides to optical applications like filters, catalyst supports, chemical sensors, biological applications, antireflection coatings in solar cells etc [17].

Among the many different Si-based materials studied for their luminescence properties, porous silicon (P-Si) has proved to be one of the most promising; as it emits light at room temperature in the visible range with high quantum efficiency. Then the properties of nP-Si structures are of increasing importance for a fundamental understanding of nanosystems as well as from a practical point of view to understand and control the materials fabrication processes [18]. Recently, a correlation has been demonstrated between the photoluminescence (PL) energy of nP-Si and the size of its remnant nanoscale silicon units.

The strong photoluminescence from nP-Si has evoked a great deal of interest due to its potential applications in optoelectronic device [19]. Thus, an in depth study of nP-Si structures may throw light on fundamental properties related to the origin of room temperature photoluminescence with quantum confinement effect and the size of the pores.

### 1.7.1 Electronic Properties

The first and most favorable explanation for the visible emission in P-Si is the quantum confinement of excitons in nanometer-sized silicon. An empirical law, based on the effective mass approximation, links the energy gap  $E_g$  of silicon nanocrystals with their sizes. The energy gap opening is given by an equal energy shift of the bottom of the conduction band to high energy and of the top of the valence band to low energy [20]. The nature of the energy-gap is still indirect even though a quasi-direct band gap can be formed in ultra small Si nanocrystals. The figure below shows the band gap variation of P-Si with size. At small size, we have a high percentage of surface atoms [21].

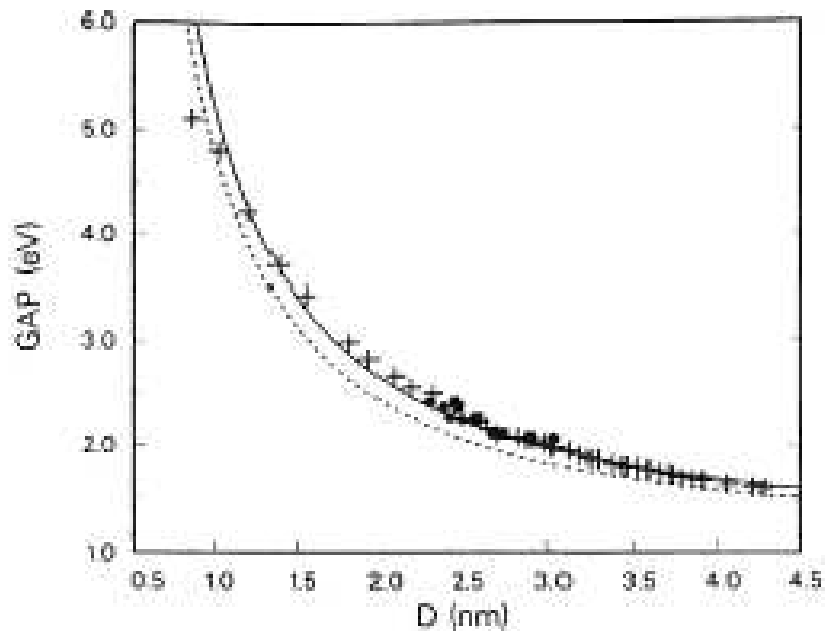


Figure.1 .6.Calculated optical gap energies for Si-crystals depending on their diameter [9, 10].

### 1.7.2 Electrical Properties

Electrical resistivity in P-Si is five orders of magnitude higher than in intrinsic Si, because P-Si is depleted by free carriers. Depletion can occur either because of the energy gap widening from quantum confinement which reduces the thermal generation of free carriers, or because of trapping of free carriers. Trapping can occur during the preparation of P-Si either because the binding energy of dopant impurities are increased or because of the formation of surface states. It has been demonstrated that the dopants are

still present in essentially unchanged concentration after the etching, but are in a neutral state. The electrical transport is mainly affected by the disordered structure of the Si skeleton, which restricts the conductive paths to a highly constrained geometry, which for certain porosities forms percolated or fractal geometry. As a consequence conductivity is thermally activated, strongly frequency dependent and highly dispersive.

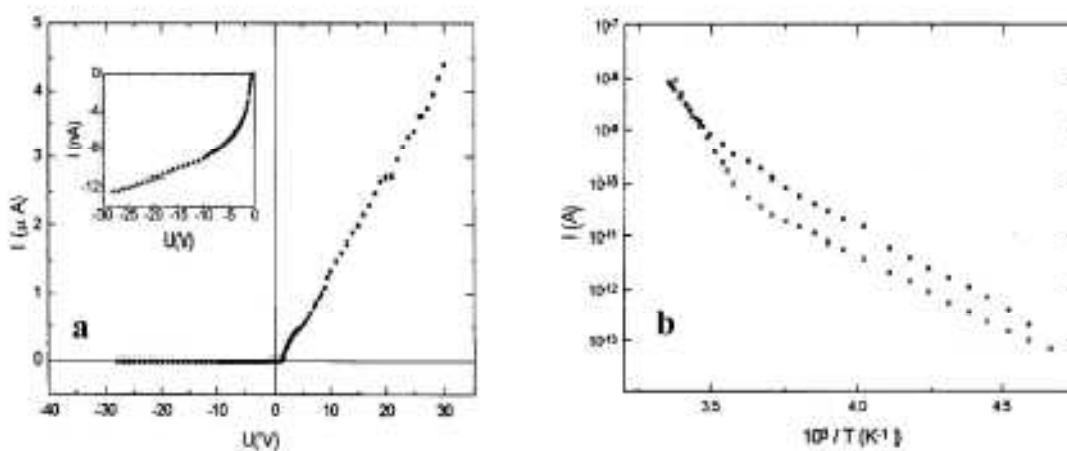


Figure.1 .7.a) I – V characteristic for oxidized P-Si samples at Room Temperature (RT); b) I – T characteristic for Oxidized P-Si samples.

### 1.7.3 Light emitting properties

Porous silicon is a form of chemical element silicon, which has an extremely large surface to volume ratio. Among the many different Si-based materials studied for their luminescence properties, porous silicon (P-Si) has proved to be one of the most promising, as it emits light at room temperature in the visible range with quantum efficiencies approaching 10% (one photon emitted for every 10 photon generated e-h pairs) [22]. Certain P-Si materials can have large photoluminescence efficiency at room temperature; a surprising result, since the PL efficiency of bulk silicon is very low due to its indirect energy band gap and short non-radiative lifetime. The reason of this was the partial dissolution of silicon, which causes: i) The formation of small silicon nanocrystals in the porous silicon material, ii) The reduction of

the refractive index of P-Si with respect to silicon, and hence an increased light extraction efficiency from P-Si and iii) The spatial confinement of the excited carriers in small silicon regions where non- radiative recombination centers are mostly absent.

**Limitations of Porous Silicon:** Devices based on porous silicon exhibit room temperature PL spectra in the visible range. However, Porous silicon has a series of disadvantages .The main striking ones are; i) Poor stability due to the high porosity and ii)The difficulty of integration of the electrochemical etching needed to produce porous silicon with the silicon VLSI (very large scale integration) technology.

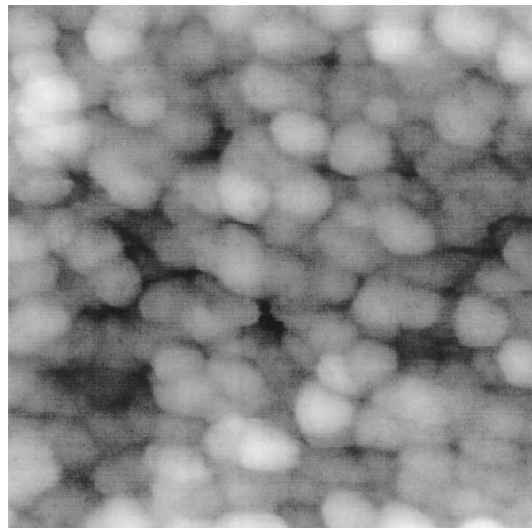


Figure.1.8. AFM image (656×656 nm) of light-emitting porous silicon [30].

## **1.8 Objectives**

### **1.8.1 General objective**

•Our main objective in this thesis is to investigate mechanism of visible light emission from nanoporous silicon quantum dot and to calculate analytically the optical properties of this material based on quantum confinement and surface state models.

### **1.8.2 Specific objective**

Specifically in this thesis we will:

- examine the effect of porosity level on energy gap, optical absorption coefficient, dielectric function and oscillator strength in nanoporous silicon quantum dot.
- investigate the main factors that make the PL peak to shift towards left or smaller wavelength.

## **1.9 Thesis outline**

Based on our objectives, in this research work, we analyze the effect of size, surface passivation and porosity level on energy gap, optical absorption coefficient, dielectric function and oscillator strength and also investigate the main factors that make to shift the PL peak towards left or smaller wavelength in nanoporous silicon quantum dot by integrating surface states and quantum confinement model to explain experimental data.

The research organized in to five Chapters. In chapter 2, we deduce the mechanism of light emission from nanoporous silicon quantum dot. In chapter 3 we discuss how the joint density of states and the dipole matrix elements are used to relate the optical absorption coefficient, oscillator strength and imaginary part of the dielectric function with the band gap and photon energy of nanoporous silicon quantum dot .We also formulate a phenomenological model to generate photoluminescence spectra of nanoporous silicon quantum dot by taking porosity level into account in the same chapter. In chapter 4, we report the results we obtained and finally, we conclude our study in the fifth chapter.

# Chapter Two

## Photoluminescence

In this chapter we are going to see types of luminescence, mechanism of visible light emission from nanoporous silicon, Photoluminescence materials and their importance.

### 2.1 Introduction

Luminescence is a general term which describes any process in which energy is emitted from a material at different wave lengths that at which it is observed. It has different meanings depending on the field of application. Therefore, there are different types of luminescence; few of them are photoluminescence, electroluminescence and cathodoluminescence.

**Photoluminescence:** by optical radiation

**Electroluminescence:** by electrical field or currents

**Cathodoluminescence:** by electron beams (cathode rays)

Luminescence resulting from the optical excitation is called photoluminescence. Photoluminescence (abbreviated as PL) is a process in which a substance absorbs photons (electromagnetic radiation) and then radiates photons back out. Quantum mechanically, this can be described as excitations to a higher energy state and then a return to a lower energy state accompanied by the emission of a photon [16] (see fig. 2.1). This is one of many forms of luminescence (light emission) and is distinguished by photo-excitation (excitation by photons), hence the prefix photo. The period between absorption and emission is typically extremely short, in the order of 10 nanoseconds. Under special circumstances, however, this period can be extended into minutes or hours. Ultimately, available chemical energy states and allowed transitions between states (and therefore wavelengths of light preferentially absorbed and emitted) are determined by the rules of quantum mechanics. A basic understanding and studying the electron configurations of the principles involved can be gained by molecular orbital of simple atoms and molecules [23].

**Electroluminescence (EL):** is an optical phenomenon and electrical phenomenon in which materials emit light in response to an electric current through it, or to a strong electric field. This is distinct from light emission resulting from heat (incandescence) from the action of chemicals (chemoluminescence), action of sound (sonoluminescence) or other mechanical actions (mechanoluminescence).

### **Mechanism**

Electroluminescence is the result of radiative recombination of electrons and holes in a material (usually semiconductors). The excited electrons release their energy as photons-light. Prior to recombination, electrons and holes are separated either as a result of doping from p-n junction (in semiconductors) luminescent devices such as LEDs, or through excitation by impact of high energy electrons accelerated by strong electric field (as with phosphorus in electroluminescent display) [25].

## **2.2 Mechanism of visible light emission from nanoporous silicon**

The recent discovery of bright visible luminescence from nanoporous Silicon has stimulated research for a better understanding of the basic mechanisms of light emission from Si nanostructures and for a better control of the numerous parameters of nanoporous silicon formation and further processing in order to give a high quantum efficiency of luminescence.

For structures related to porous silicon, Canham showed that the confinement requirements can be obtained by chemical dissolution of porous samples. Related to chemical thinning of crystallites, a blue shift of the fluorescence was also observed. It is suggested that passivation is provided by hydrogenation during the dissolution, but spontaneous oxidation when samples are exposed to air could not be excluded as a perturbation to the passivation. Some previous works have shown that visible luminescence could be obtained from as-formed high-porosity samples without further chemical dissolution and that an enhanced emission is observed after anodic oxidation. This complementary process has the advantage of bestowing good mechanical properties on the porous layer. In addition it gives rise to a bright electroluminescence [24].

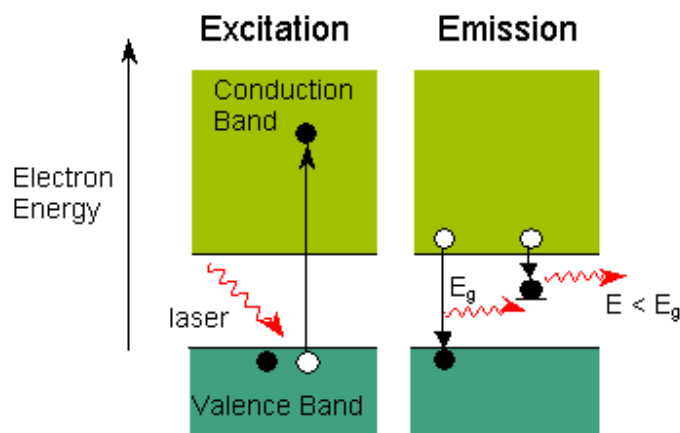


Figure .2.1. Photoluminescence. On the left a high energy laser photon gets out an electron from its orbit. The electron loses energy until it reaches the bottom of the conduction band. The right hand diagram shows two possible transitions. On the left the electron combines immediately with a hole in the valence band emitting a photon of energy  $E_g$ . On the right it gets stuck in a 'between-gap' state emitting a lower energy photon [34].

## 2.3 Examples of photoluminescence materials

The process of manufacturing photoluminescent material can be described as a sol-gel process. It is aligned with the principles of green chemistry.

Photoluminescent materials have existed in many forms, some occurring naturally in the form of phosphorescent inorganic minerals in the earth. A series of special minerals, amongst others, which give rise to the phenomenon of photoluminescence are known as the lanthanide series of elements in the periodic table. The lanthanides belong to a group commonly known as rare earths. The unique electronic structure of these elements with f-electrons and partially filled d-levels offer an excellent opportunity to create electron triplet states with long lifetimes. These states in turn give rise to phosphorescence.

When very small amounts of compounds such as oxides, halides, nitrates, etc of these lanthanide elements are amalgamated with selected inorganic compounds and sintered under controlled heat and atmospheric conditions, the result can be a photoluminous material. Such material absorbs energy from

radiant sources when exposed to them, and emits this energy in the form of luminous photons over a long period when compared to the short exposure time. The following are photoluminescence materials.

- Zinc sulphide
- Aluminates of calcium and strontium doped with rare earth elements.
- Strontium aluminate crystals doped with two rare earth elements.

The addition of rare earth elements is to give an improved intensity of illumination over a longer period when compared to zinc sulphide.

It is desirable to produce an improved photoluminescent material with persistent after-glow characteristics and particularly in which the rate of decay of the afterglow is reduced relative to traditionally used photoluminescent material, such as zinc sulphide. Reduced rate of decay has become a desirable characteristic as it results in photoluminescent material that can maintain persistent after-glow for longer periods [12].

## **2.5 Importance of photoluminescence materials**

Nanocomposite materials of suitable composition have also been known for some time for their non-linear optical properties and for their luminescence. Nanocomposite photoluminescent materials have a potential application as light sources, and the ones based on silicon, if their production proves to be compatible with silicon technology, may be used in electronic devices as well. Possible uses in the optoelectronic field are also foreseen for these materials, thanks to the possibility of modulating the dielectric properties of silica or of enhancing the emission properties of radiative centers, such as  $\text{Er}^{3+}$  ions in silica. It is also studied the possible use of these materials for the production of extremely high density memories, through the realization of single-electron transistors, wherein the electron is confined in a space having dimensions of few nanometers buried in an insulating matrix, for instance silica,  $\text{SiO}_2$  [14].

In an even further aspect, a use of said long-decay photoluminescent material in long after-glow products has been discovered. The products include paints, extrudable and moldable plastics and/or dispersions. Solvent based paints, ceramics, coatings, moulded ceramic glazes and the like. In particular, due to the incorporation of silicate into the complex, the photoluminescent material of this type is suited for nanostructures [13].

## Chapter Three

### Optical behavior of nanoporous silicon quantum dot

In this chapter we are going to derive an expression for optical parameters (absorption coefficient, dielectric constant and oscillator strength). We will also see the effect of temperature on these optical parameters and surface effects on photoluminescence. Finally we will generate a model for photoluminescence which helps us to derive an expression for photoluminescence intensity

#### 3.1 Optical parameters

Optical parameters include density of state, absorption coefficient, dielectric constant, oscillator strength, refractive index, non radiative life time, radiative life time, exciton, optical thickness (nd), etc. In the coming subsections we will see the relation between these optical parameters (optical absorption coefficient, dielectric constant and oscillator strength) with nanoporous silicon quantum dot diameter (size) through energy gap.

##### 3.1.1 Absorption coefficient

The optical absorption coefficient is proportional to the number of optical transitions per unit volume and time elements. Therefore, it can be given by the absorption energy per unit time,  $\hbar\omega W(\omega)$ , divided by the energy flux,

$$\left( \frac{A_0 W^2 \epsilon_0 n_r}{2c\pi} \right),$$

$$\text{i.e. } \alpha(\omega) = \frac{\hbar\omega W(\omega)}{A_0^2 \omega^2 \epsilon_0 \frac{n_r}{2c\pi}} \quad (3.1.1)$$

The total number of optically induced transitions per unit volume and unit time can be given as:

$$W(\omega) = \frac{2\pi}{\hbar} \left( \frac{eA_0}{m_0c} \right)^2 |\hat{e} \cdot M_{cv}(k)|^2 J_{cv} \quad (3.1.2)$$

Where, the Joint Density of State  $J_{cv}$  can be expressed as:

$$J_{cv} = \frac{1}{2\pi^2} \left( \frac{2m_r^*}{\hbar^2} \right)^{\frac{3}{2}} \sqrt{\hbar\omega - E_g} \quad (3.1.3)$$

Here  $J_{cv}$  related to energy gap which is a function of size. Therefore, the absorption coefficient near the absorption edge will be:

$$\alpha(\omega) = \frac{4\pi^2 e^2}{\epsilon_0 n c m_0^2 \omega} \{ |\hat{e} \cdot M_{cv}|^2 J_{cv} \} \quad (3.1.4)$$

Using eq. (3.1.3),

$$\alpha(\omega) = \frac{4\pi^2 e^2}{\epsilon_0 n c m_0^2 \omega} \{ |\hat{e} \cdot M_{cv}|^2 \left( \frac{1}{2\pi^2} \left( \frac{2m_r^*}{\hbar^2} \right)^{\frac{3}{2}} \sqrt{\hbar\omega - E_g} \right) \}$$

$$\alpha(\omega) = \left\{ \frac{2e^2 (2m_r^*)^{3/2}}{\epsilon_0 n c m_0^2 \hbar^2 \omega} \right\} |\hat{e} \cdot M_{cv}|^2 \sqrt{\hbar\omega - E_g}$$

The matrix element is given by:

$$|\hat{e} \cdot M_{cv}|^2 = \frac{3}{2} \frac{m_0}{m_r^*} (m_0 - m_r^*) \frac{E_g + \Delta_0}{3E_g + 2\Delta_0} E_g \quad (3.1.5)$$

Hence,

$$\alpha(\omega) = \frac{3e^2\sqrt{m_o}}{\varepsilon_o n \hbar^2 c} \left(\frac{2m_r^*}{m_o}\right)^{\frac{3}{2}} \frac{m_o - m_e^*}{m_e^*} \frac{E_g + \Delta_o}{3E_g + 2\Delta_o} \frac{E_g}{\hbar\omega} \sqrt{\hbar\omega - E_g}$$

$$\alpha(\omega) = \frac{3e^2\sqrt{m_o}}{\varepsilon_o n \hbar^2 c} \left(\frac{2m_r^*}{m_o}\right)^{\frac{3}{2}} \frac{m_o - m_e^*}{m_e^*} \frac{E_g}{\hbar\omega} f(g) \quad (3.1.6)$$

Where:  $f(g) = \frac{E_o + \Delta_o}{3E_o + 2\Delta_o} \sqrt{\hbar\omega - E_g}$

For  $\hbar\omega \approx E_g$

$$\alpha(\omega) = 0 \quad (3.1.7)$$

From eq. 3.1.6 we can see that the optical absorption coefficient is function of photon energy and energy gap. But Zunger et al using tight-binding method, Tripathy et al and Ghoshal et al using local pseudopotential method calculate the bandgap energy as a function of diameter (size) for clean and passivated surface silicon nanoclusters at room temperature. As a result even if the optical absorption coefficient is directly a function of energy gap and photon energy it is indirectly a function of silicon nanoclusters diameter (size) through the band gap.

### 3.1.2 Dielectric function

For semiconductor with optical absorption  $\alpha$ , the refractive index is complex and given by

$$\tilde{n} = n_r + ik \quad (3.1.8)$$

This complex index of refraction is related to the complex dielectric constant as

$$\tilde{\epsilon} = \epsilon' + i\epsilon'' \quad (3.1.9)$$

Where:  $\epsilon' = \epsilon$

$$\epsilon'' = \frac{\sigma}{\epsilon_0 \omega}$$

From eq. (3.1.8) and eq. (3.1.9), we will get

$$\epsilon' = n_r^2 - k^2$$

$$\epsilon'' = \frac{\sigma}{\epsilon_0 \omega} = 2n_r k$$

But the optical absorption coefficient is given by

$$\alpha = \frac{2\omega k}{c} \Rightarrow k = \frac{c\alpha}{2\omega}$$

$$\epsilon'' = \frac{\alpha c n_r}{\omega} \quad (3.1.10)$$

And using eq. (3.1.6)

$$\epsilon'' = \frac{3e^2\sqrt{m_0}}{\epsilon_0\hbar^2\omega} \left(\frac{2m_r^*}{m_0}\right)^3 \frac{m_0 - m_e^*}{m_e^*} f(g) \quad (3.1.11)$$

$$\text{Where, } f(g) = \frac{E_g + \Delta_0}{3E_g + 2\Delta_0} \sqrt{\hbar\omega - E_g}$$

As we can see from eq. 3.1.11 the imaginary part of the dielectric function is directly a function of energy gap and photon energy while it is indirect function of silicon nanoclusters diameter (size) through the band gap.

### 3.1.3 Oscillator strength

The Oscillator strength, the equivalent number of oscillations of the transition between the valance and conduction bands, is related to the matrix element of the momentum matrix  $P_{cv}$  and is given by the equation:

$$f_{cv} = \frac{2|P_{cv}|^2}{m_0\hbar\omega_{cv}} \quad (3.1.12)$$

Where  $P_{cv} = |\hat{e} \cdot M_{cv}|$

$$\Rightarrow f_{cv} = \frac{2|\hat{e} \cdot M_{cv}|^2}{3m_0\hbar\omega_{cv}} \quad (3.1.13)$$

The factor  $\frac{1}{3}$  in the above equation is due to averaging with  $|M_x|^2 = |M_y|^2 = |M_z|^2 = \frac{|M|^2}{3}$ .

And in equation (3.1.5) we see that

$$|\hat{\mathbf{e}} \cdot \mathbf{M}_{cv}|^2 = \frac{3 m_o}{2 m_e^*} (m_o - m_e^*) \frac{E_g + \Delta_o}{3E_g + 2\Delta_o} E_g$$

Inserting this equation in to equation (3.1.12) and using  $m_e = 0.4m_o$  we obtain:

$$f_{cv} = \frac{2}{3m_o \hbar \omega_{cv}} \frac{3 m_o}{2 m_e^*} (m_o - m_e^*) \frac{E_g + \Delta_o}{3E_g + 2\Delta_o} E_g \quad (3.1.14)$$

$$f_{cv} = \frac{3}{2m_o \hbar \omega_{cv}} \frac{E_g + \Delta_o}{3E_g + 2\Delta_o} E_g \quad (3.1.15)$$

From eq. 3.1.15 we can see that the oscillator strength is directly a function of energy gap and photon energy while it is indirect function of silicon nanoclusters diameter (size) through the band gap.

## 3.2 Effect of temperature on the optical properties of porous silicon

Temperature is a critical parameter which affects the optical properties of porous silicon. As the etching temperature decreases, the refractive index ( $n$ ) decreases, indicating a higher porosity and the physical thickness of PS samples also decreases. Meanwhile, the reflectance spectra exhibit a more intense interference band and the interfaces are smoother. In addition, the intensity of the PL emission spectra is dramatically increased. The photoluminescence (PL) of porous silicon (PS) at room temperature discovered in 1990 by Canham *et al.* has stirred a wide variety of interests in its potential applications, including light emitting devices, sensors, and optical microcavities. Especially, in 1996, the realization of silicon-based visible light-emitting prototype devices integrated into microelectronic circuits was a milestone for the applied researches of PS. It has been well established that many parameters of PS, such as the emission intensity, the porosity, the refractive index, the thickness, the uniformity, the smoothness of the surface and interface, the pore diameter, and the microstructure, on which the PL of PS depends, are strongly dependent on the anodization condition, which includes the composition of the electrolyte, the current

density, the etching time, and the conduction type and resistivity of a Si wafer as well. Therefore, many researches have focused on the effects of anodic parameters on the properties of PS, resulting in a lot of valuable experimental results. However, these researches were mostly carried out at room temperature, and the effects of the etching temperature on the microstructure and photoluminescence characteristics of PS have scarcely been studied. Nevertheless, Ono *et al.* reported the effects of the etching temperature on the photoluminescence spectra of PS, showing that a decreasing etching temperature results in a decrease of the photoluminescence intensity of PS. However, an inverse result was observed by Setzu *et al.* More recently, Blackwood *et al.* reported that PL intensities varied randomly. Furthermore, the red-shift of the PL peak wavelength with the decreasing etching temperature was observed by Ono *et al.*, while oppositely Blackwood *et al.* observed a blue-shift trend. Although the above researches have not revealed any correlating rules, they did show the strong dependence of the PL intensity on the etching temperature. In 2002, Reece *et al.* fabricated high-quality PS optical micro-cavities with the electrolyte temperature kept at  $-22.5\text{ }^{\circ}\text{C}$ . The optical resonance of the micro-cavities operating in the near infrared range had a line-width of 0.63 nm, while other reports have shown PS microcavities fabricated at room temperature operated with the full width at half maximum (FWHM) of 6–15 nm. The optical micro-cavities prepared at  $-22.5\text{ }^{\circ}\text{C}$  clearly demonstrate that the etching temperature is a key factor for preparing the high-quality PS multilayers. It is well known that the quality of the PS optical devices, such as micro-cavities and Bragg reflectors (DBRs), is determined by the uniformity of the PS layer and the interface smoothness. Therefore, it is necessary to systemically investigate the relationship between the smoothness of a PS interface and the etching temperature. The results of previous work by Long Yongfu *et al.* demonstrate that the interface smoothness and the optical properties of PS strongly depend on the solution temperature of anodization. At a constant current density of  $140\text{ mA/cm}^2$ , when the etching temperature decreased from 50 to  $-40\text{ }^{\circ}\text{C}$ , the formation rate of PS was reduced by 55%, resulting in a more uniform layer and smoother interfaces; meanwhile, the optical thickness ( $nd$ ) decreased by almost three quarters. In addition, the PL intensity of PS increased by two orders of magnitude as the temperature decreased from 18 to  $-40\text{ }^{\circ}\text{C}$ , and a red-shift of the PL peak wavelength was observed [26].

### 3.3 Effect of surface states on photoluminescence

When the valence electrons  $3s^2 3p^2$  of a silicon atom form hybrid orbitals  $sp^3$  to make bonds with neighboring atoms, their energy levels split into bonding and antibonding states. The valence electrons

have accommodated in the bonding state, so the anti-bonding state is empty. Since in a crystal many atoms make bonds with each other to arrange themselves periodically, these energy levels have broadened to make bands: the valence band and the conduction band, respectively. These are electronic states in a bulk crystal. However, on the surface there exist dangling bonds (unpaired hybrid orbitals), which are similar to the hybrid orbitals of isolated atoms, whose energy levels will be located between the bonding and antibonding states, or within an energy gap (see figure 3.1).

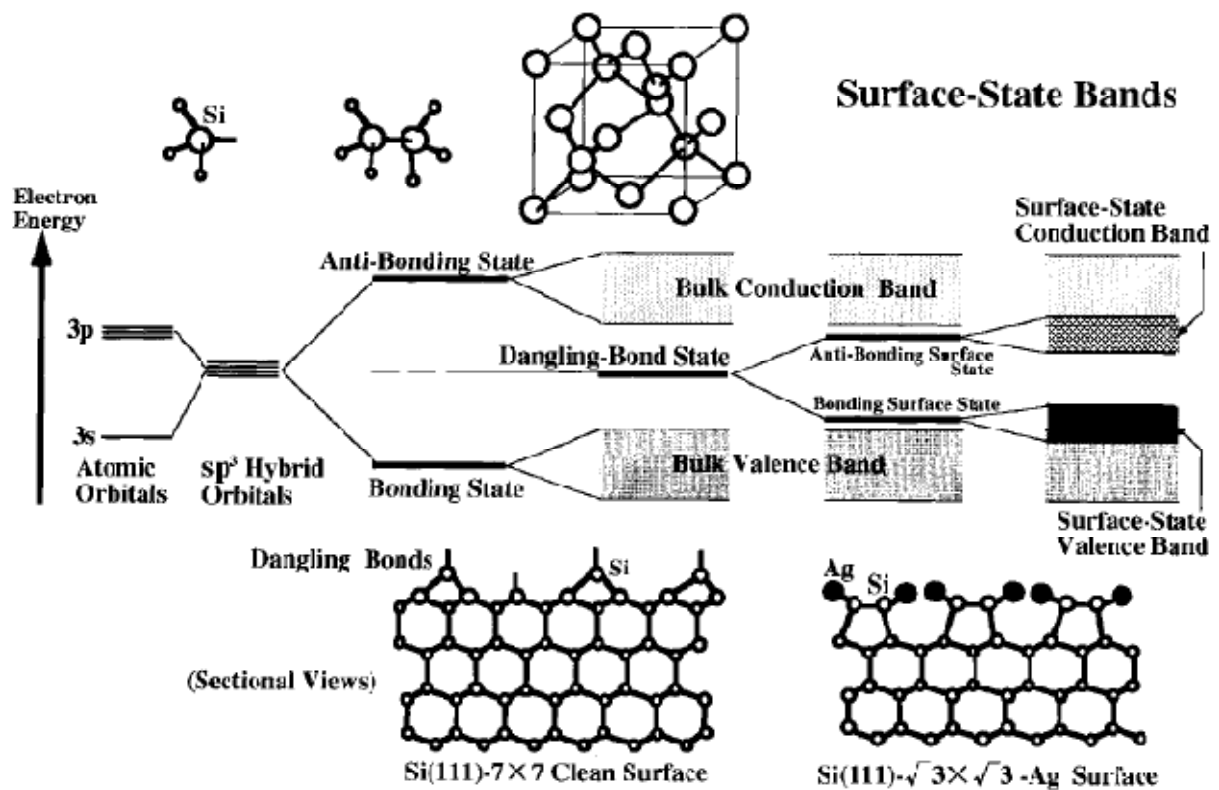


Figure.3.1. A schematic energy diagram for atoms and molecules, and also the bulk and the surface of a silicon crystal [27].

In fact, the dangling-bond state on a clean Si (111) surface is known to lie around the middle of the band gap [27]. In addition, surface to volume ratio increase as the crystallite size decreases hence; the influence of surface states on the photoluminescence from smaller crystallites will be highly enhanced. Therefore, the

role of surface states, especially for low crystallite size should be included into account during the study of photoluminescence mechanism. Wolkin et al. obtained photoluminescence spectra at room temperature by using a pulsed excitation nitrogen laser (337 nm) and/or a continuous excitation HeCd laser (325nm) [28]. Accordingly, figure 3.2 (a) shows the photoluminescence spectra of five types of

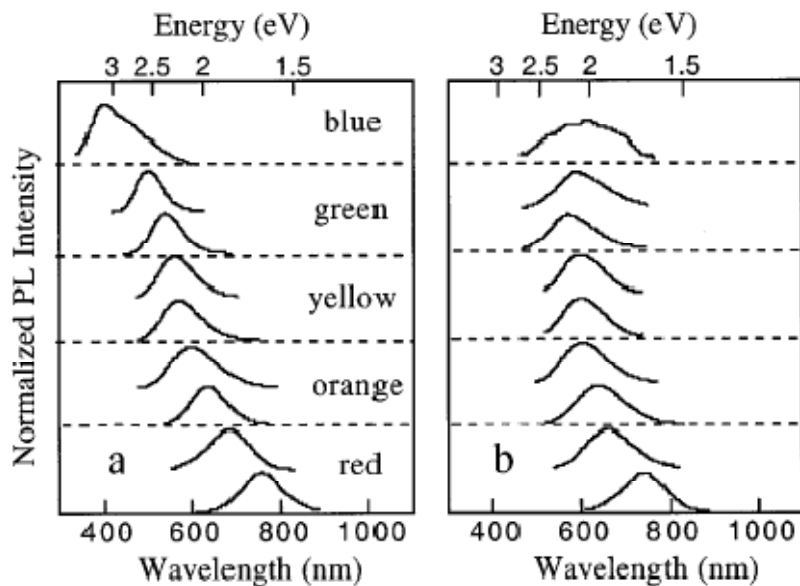


Figure.3.2. Room temperature photoluminescence spectra from porous silicon samples with different porosities kept under Ar atmosphere (a) and after exposure to air (b) [27].

Oxygen-free porous silicon samples with different porosities. Stable red, orange, yellow, green and blue spectra have observed as increasing the order of porosity. The results have obtained and measured during the samples kept in the Ar environment. Where as, figure 3.2 (b) shows how the spectra were modified after the samples had been exposed to air for 24 h and they observed that oxidation introduces states in the band gap which pin the transition energies. In addition, below about 3nm in size, oxide passivated nanocrystals are luminescence at lower energy than hydrogen passivated nanocrystal [29]. Calculation shows that the size of the bandgap and the corresponding spatial pattern of the highest occupied molecular orbital (HOMO) and lowest unoccupied molecular orbital (LUMO), depend upon the electronegativity of the passivating layer at such small size. In oxide, terminated nanocrystals the HOMO is sketch to the

surface and resides in weakened Si - Si back bonds on interfacial Si atoms directly bonded to oxygen. Therefore, we realized that as the silicon exposed to air oxygen make a bond with the dangling bond and the SiO<sub>2</sub> layer cover the surface as shown in figure 3.3, the same is true when the dandling bond makes a bond with Hydrogen, and surface states appears in the band gap. Consequently, the photoluminescence peak shifted (modified) due to surface states. Therefore, surface passivation has remarkable effect on photoluminescence intensity.

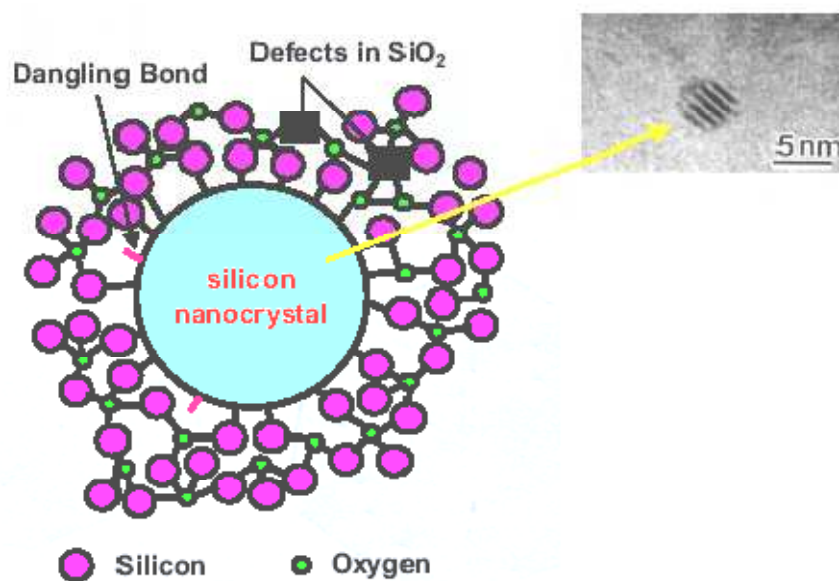


Figure.3.3. Silicon nanocrystals embedded in SiO<sub>2</sub> [29].

We formulate a model for photoluminescence intensity by taking the effect of surface and exciton states into account in the coming section. In addition, we give a quantitative expression for the photoluminescence intensity [29].

### 3.4 Formation of a model to generate photoluminescence spectra

The study of nanoporous silicon quantum dot is a very active field of research due to the interesting fundamental physical properties and the promising applications in advanced electronic and optoelectronic

devices [23]. The optical properties have been studied intensively for frequencies near the fundamental energy gap of the dots with respect to photoluminescence. Here we are going to formulate and describe the photoluminescence spectra from nanoporous silicon quantum dot. To do so, let us consider nanoporous silicon quantum dot as an ensemble of having a well defined size distribution function  $n(d)$ . On excitation with high-energy photons, photocarriers have generated inside the crystallites and then a fraction of these photoexcited carriers relax non-radiatively to the surface states. Subsequently, the relaxed carriers recombine to ground states radiatively giving photoluminescence. So, the intensity of photoluminescence at particular photon energy becomes proportional to the population of occupied surface states and the oscillator strength. The number of surface states  $N_s$  in a quantum dot is proportional to the number of atoms on the surface and hence, surface area  $A$  of the quantum dot. Additionally, if we assume that each atom in a quantum dots contributes at least one photoexcited carrier to the quantum dot, the number of photoexcited carriers  $N_v$  in the quantum dot is proportional to its volume,  $V$ . The rate of transition from an excited carrier to the localized surface states is proportional to the product of the number of excited photocarriers and the number of available empty surface states in steady state condition, the population  $N_r$  of photocarriers in surface states participating in photoluminescence processes becomes proportional to the product, i.e.

$$N_r \sim AV \quad (3.4.1)$$

For a quantum dot of diameter  $d$  we have  $V \sim d^{3-\beta_1}$  and  $A \sim d^{2-\beta_2}$ . So we get

$$N_r \sim d^{5-(\beta_1+\beta_2)} \quad (3.4.2)$$

Where  $\beta_1$  and  $\beta_2$  are porosity parameters and are less than one .In the strong confinement regime, blue shift in band gap energy is quite significant compared to weak confinement limit. Along with the blue shift of the band gap and excitonic levels, particle size reduction also causes an enhancement in the oscillator strengths ( $f$ ). This can be understood as follows: optical transition probability in a bulk semiconductor is proportional to the probability of finding an electron and a hole in the same unit cell of the crystal. Hence, the oscillator strength of the exciton  $f_{ex}$  is inversely proportional to  $a_B^3$ . In the case of quantum dot

transition probability is proportional to the spatial restriction of carrier motion in the quantum dot volume due to externally imposed quantum confinement, i.e. [31]

$$f \sim \frac{1}{d^{3-\beta_3}}$$

$\beta_3$  also defined in the same way as  $\beta_1$  and  $\beta_2$ . Now, taking the oscillator strength into account, the radiative transition probability in a quantum dot of diameter  $d$  becomes

$$P(d) \sim f N_r \sim d^{2+\beta_3-(\beta_1+\beta_2)} \quad (3.4.3)$$

Now, the photoluminescence intensity from an ensemble of quantum dot size  $d$  having size distribution  $n(d)$  will be given by

$$I(d) \sim P(d) n(d) \quad (3.4.4)$$

The emitted photon energy from the quantum dot should be lower than the bandgap energy of quantum confinement model by an amount of the localization binding energy  $E_s$  of the surface states and the exciton binding energy  $E_b$ . Hence, the emitted photon energy from quantum dot will be:

$$E_{pl} = E_g^{bulk} + \Delta E - E_b - E_s \quad (3.4.5)$$

According to quantum confinement model the band gap up shift can be modeled  $\Delta E = \beta/d^\gamma$  where  $\beta$  and  $\gamma$  are constants due to quantum confinement effect, their magnitudes strongly depend up on the band gap calculation method being employed. We transform Eq. 3.4.4 from  $d$  to  $\Delta E$  dependence as

$$I(\Delta E) = \int I(d)n(d)\delta\left(\Delta E - \frac{\beta}{d^\gamma}\right) dd \quad (3.4.6)$$

Where  $dd$  means integration with respect to  $d$  as  $dx$  which is integration with respect to  $x$ .

Taking

$$n(d) = \frac{1}{\sigma\sqrt{2\pi}} \exp\left(-\left(\frac{d-d_0}{2\sigma}\right)^2\right)$$

Where  $d_0$  and  $\sigma$  are the mean dot size and standard deviation respectively. So, we obtained an expression for the photoluminescence intensity as:

$$I(\Delta E) \sim \frac{1}{\sigma\sqrt{2\pi}} \left(\frac{\beta}{\Delta E}\right)^{\frac{2}{\gamma}} \exp\left[-\frac{\left\{\left(\frac{\beta}{\Delta E}\right)^{\frac{1}{\gamma}} - d_0\right\}^2}{2\sigma^2}\right] \quad (3.4.7)$$

Eq. 3.4.7 gives general expression for photoluminescence intensity from nanoporous silicon quantum dots ensemble. It is clear from the above expression is that the photoluminescence intensity depends strongly on the quantum confinement parameters  $\beta$  and  $\gamma$ . We took  $\gamma = 1.32$  and  $1.42$  to plot two graphs for these two values of  $\gamma$  which will be discussed in chapter four,  $\beta = 3.73$  eV and  $E_g^{bulk} = 1.12$  eV at room temperature. The localization binding energy  $E_s$  has taken to be the order of phonon energies, which is about 0.05eV for optical phonons. It is important to note that earlier researchers have taken oscillator strength as proportional to  $\frac{1}{d^\gamma}$  but we used  $\frac{1}{d^{3-\gamma}}$

## Chapter Four

### Model, Results and Discussions

In chapter three we have seen how the optical absorption coefficient, the dielectric function and oscillator strength are related to size of nanoporous silicon quantum dot through energy gap. We have also found the expression for photoluminescence intensity from silicon quantum dots ensemble. The aim of this thesis also extends to the dependence of energy gap of nanoporous silicon quantum dot on the size of the dot. Here in addition to their size dependence we also take into account the effect of porosity level and surface passivation. Therefore, in this chapter we investigate the results based on our expressions. The plots are generated from the relations we obtain in equations (1.5.13), (3.1.6), (3.1.11), (3.1.15) and (3.4.7) using MATLAB programs.

According to many calculations and observations, the optical energy gap (eq. 1.5.13) is given as:

$$E_g^{nano} = E_g^{bulk} + \frac{c}{d^\alpha} \quad (4.1)$$

Where  $E_g^{nano}$  and  $E_g^{bulk}$  are the band gap energies of silicon nanoporous quantum dot and bulk silicon respectively,  $d$  is size of silicon nanoporous quantum dot and the values of  $c$  and  $\alpha$  depend on the nature of the surface as well as the symmetry of nanoclusters.

For pure sample at room temperature eq. (4.1), becomes:

$$E_g^{nano} = E_g^{bulk} + \frac{3.73}{d^\alpha} \quad (4.2)$$

And, for hydrogen and oxygen passivated respectively it becomes:

$$E_g^{nano} = E_g^{bulk} + \frac{4.042}{d^\alpha} \quad (4.3)$$

$$E_g^{nano} = E_g^{bulk} + \frac{3.82}{d^\alpha} \quad (4.4)$$

In addition to varying size of nanoporous silicon quantum dot, varying porosity level of the material and see its effect on energy gap and optical parameters (absorption coefficient, dielectric function and oscillator strength) of nanoporous silicon quantum dot is the main objective of this thesis. Therefore, let us take two different values for  $\alpha$  ( $\alpha = 1.32$  and  $1.42$ ) in the above equations.

Now using eq. (4.2), eq. (4.3) and eq. (4.4) together with effective mass of hole,  $m_h^* = 0.54m_0$ , effective mass of electron,  $m_e^* = 0.4m_0$ , bulk silicon spin-orbit splitting,  $\Delta_o = 0.044\text{eV}$ , effective refractive index of porous silicon nanocluster (quantum dot),  $n_r = 1.7$  and taking the value of photon energy in eq. (3.1.6), (3.1.11) and (3.1.15) as,  $\hbar\omega = 3\text{eV}$  we can finally get the optical absorption coefficient for porous silicon nanoclusters (quantum dot) with size (1-10nm) from eq. (3.1.6) as:

$$\alpha = 5.15 \times 10^5 \times (E_g) \left( \frac{E_g + 0.044}{3E_g + 0.088} \right) \sqrt{3 - E_g} \text{ eV}^{-1/2} \text{ cm}^{-1} \quad (4.5)$$

Where the imaginary part of the dielectric function from eq. (3.1.11), becomes:

$$\varepsilon'' = 10.22 \times (E_g) \left( \frac{E_g + 0.044}{3E_g + 0.088} \right) \sqrt{3 - E_g} eV^{1/2} \quad (4.6)$$

And finally the oscillator strength from eq. (3.1.15) becomes:

$$f = \left( \frac{1}{2m_o} \right) \left( \frac{E_g + 0.044}{3E_g + 0.088} \right) E_g \quad (4.7)$$

In the next sections based on the above derived expressions (eqs.4.1 -4.7) we will plot them using MATLAB programs and understand them in detail.

## **4.1 Dependence of optical energy gap on porosity parameters $c$ and $\alpha$ of nanoporous silicon quantum dot**

In this section we describe analytically the behavior of optical energy gap of nanoporous silicon quantum dot as a function of its level of porosity and size. Taking  $E_g^{bulk} = 1.12\text{eV}$ ,  $c = 4.5$  and  $6.2$ ,  $\alpha = 1.32$  and  $1.42$ , where  $c$  and  $\alpha$  are called porosity parameters and varying  $d$  from  $1\text{nm}$  to  $10\text{nm}$  in eq. (4.1), the following figures (figure 4.1 and figure 4.2) can be obtained. As we can see from these figures, the energy gap of silicon nanoporous quantum dot increases as its size decreases. In addition, the variation of energy gap was also observed by varying porosity level and we found that energy gap decreases with increasing the value of  $\alpha$  and it increases with increasing value of  $c$  (see figures 4.1 and 4.2 carefully). Our results are in good agreement with recent experimental and theoretical findings.

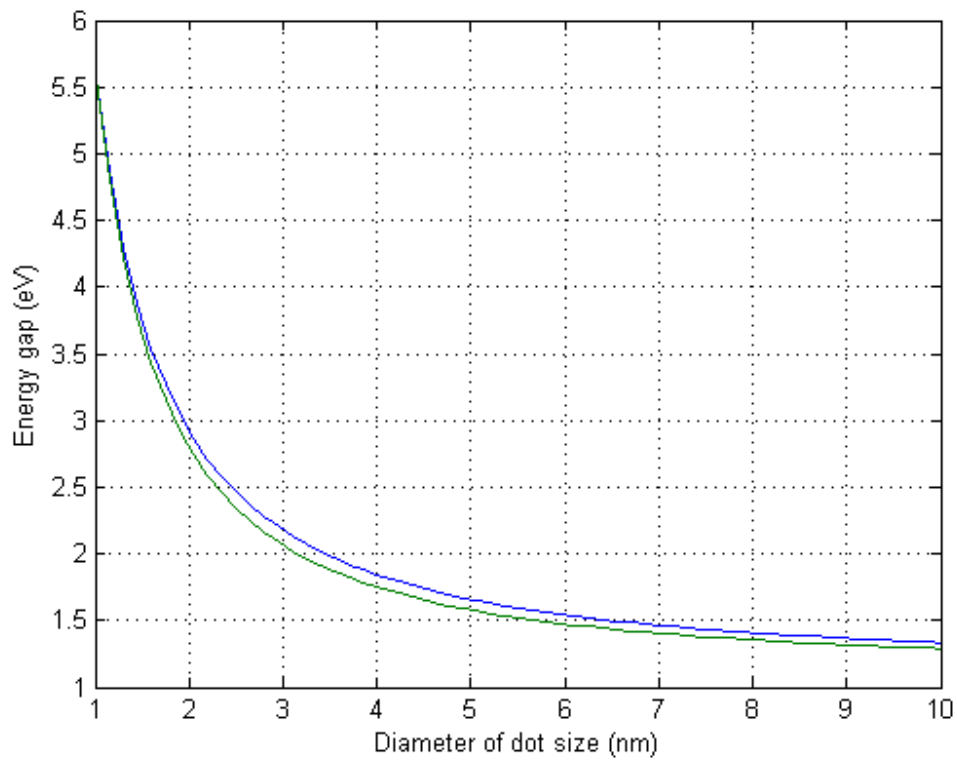


Figure .4.1. Variation of optical energy gap with porous silicon nanocluster (quantum dot) diameter. The upper line (blue) is for  $\alpha = 1.32$  (10% to 20% porosity) and the lower line (green) is for  $\alpha = 1.42$  (30% to 40% porosity). For both lines  $c = 4.5$ .

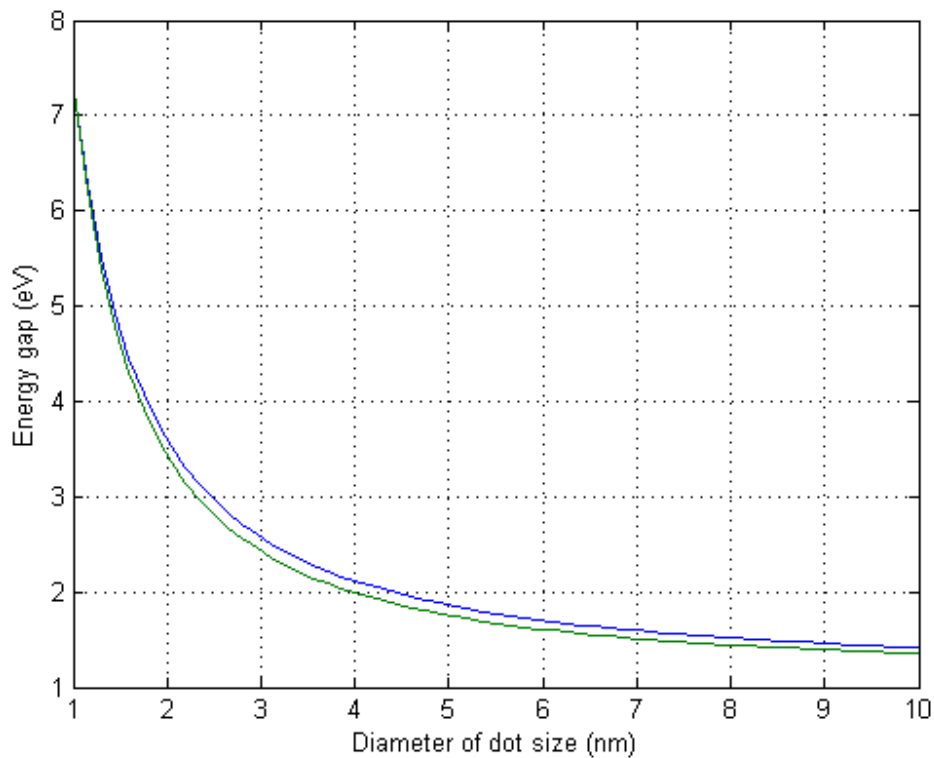


Figure .4.2. Variation of optical energy gap with porous silicon nanocluster (quantum dot) diameter. The upper line (blue) is for  $\alpha = 1.32$  (10% to 20% porosity) and the lower line (green) is for  $\alpha = 1.42$  (30% to 40% porosity). For both lines  $c = 6.2$ .

## 4.2 Dependence of optical absorption coefficient on porosity level of nanoporous silicon quantum dot

In this section we explain how Optical absorption coefficient varies by taking size of nanoporous silicon quantum dot, its porosity level and surface passivation into account. Using eq. (4.2-4.5) the plot of optical absorption coefficient versus effective size (1-10 nm) for clean, hydrogen and oxygen passivated porous silicon nanoclusters (quantum dot) at a given photon energy (3eV) and  $\alpha = 1.32$  is shown in fig.4.3 whereas for other value of  $\alpha$  i.e. when  $\alpha = 1.42$ , the plot is shown in fig.4.4.

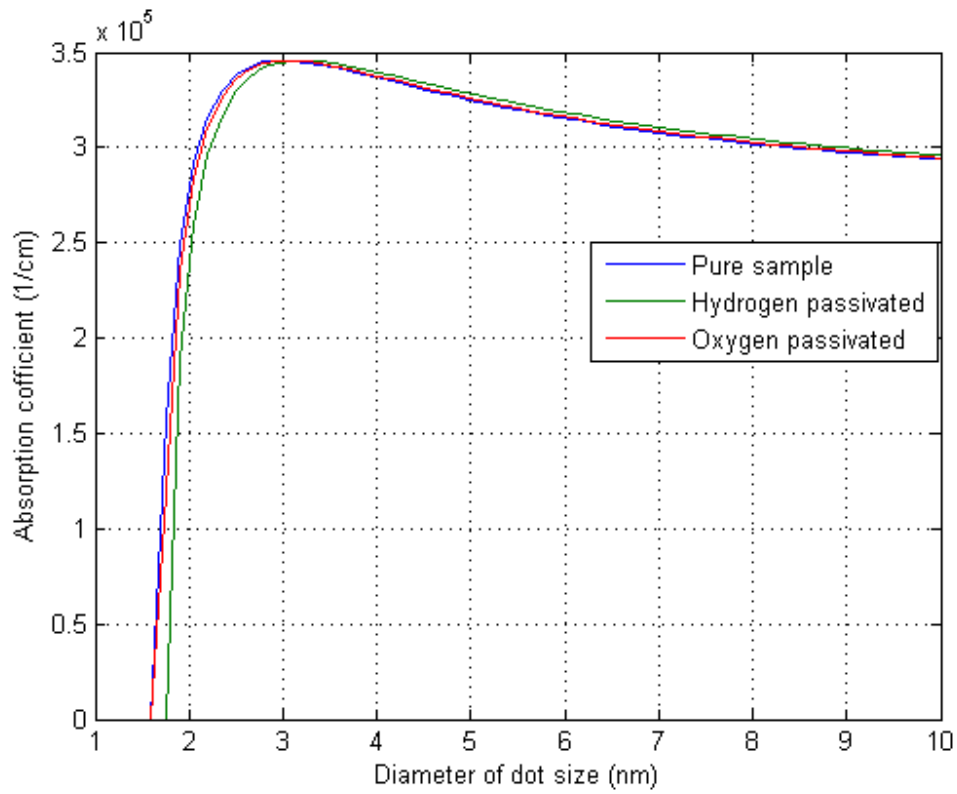


Figure.4.3. Optical absorption coefficient as a function of porous silicon nanocluster (quantum dot) size at a given photon energy  $\hbar\omega=3\text{eV}$ . For both pure and passivated samples  $\alpha = 1.32$  (10% to 20% porosity).

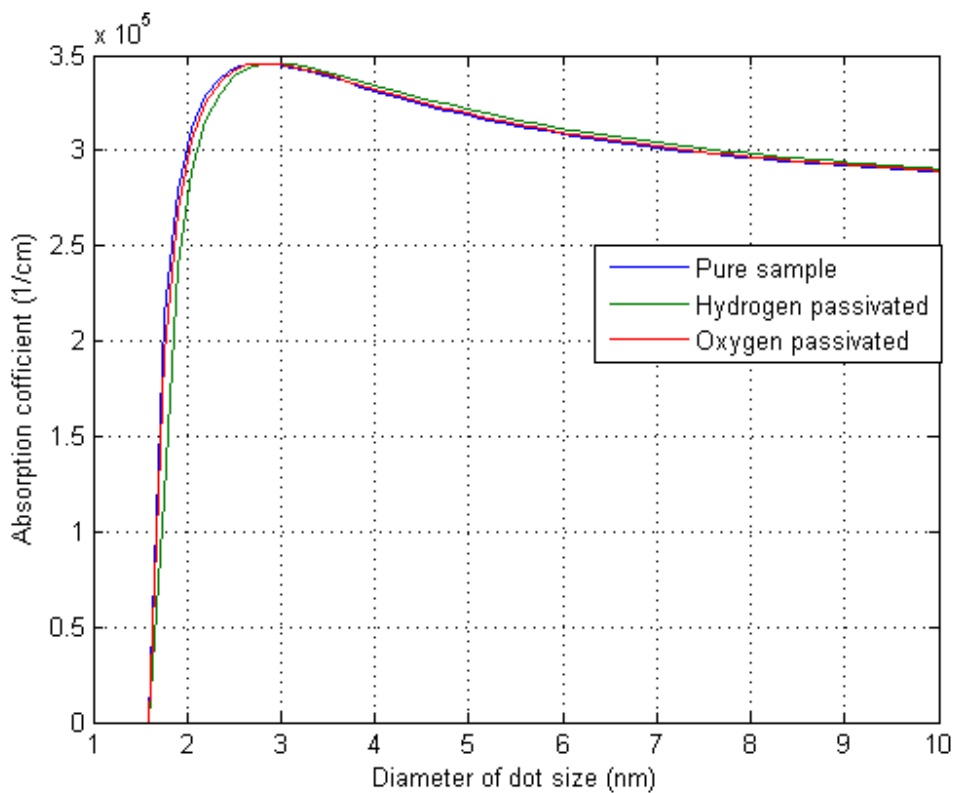


Figure.4.4. Optical absorption coefficient as a function of porous silicon nanocluster (quantum dot) size at a given photon energy  $\hbar\omega=3\text{eV}$ . For both pure and passivated samples  $\alpha = 1.42$  (30% to 40% porosity).

We have verified that the optical absorption coefficient of nanoporous silicon quantum dot strongly depends not only on the size of the nanoparticles (quantum confinement), but also on the surface passivation and porosity level. We observed that the effect of both size of the nanoparticles (quantum confinement) and the surface passivation on optical absorption coefficient is dominant at very small size

(~1.5-2.5 nm). The reason for these two effects to be dominant at very small size is due to large volume fraction of the near surface region over the crystalline core (surface effect) and position of carriers is largely confined (quantum confinement effect). In this very small region optical absorption coefficient increases rapidly with increasing size. But as we keep on increasing the size, both the surface and quantum confinement effects play very little role on the absorption coefficient and it is found that the optical absorption coefficient decreases for increasing nanoparticles diameter. By careful observation and comparison of two figures (fig .4.4& fig.4.5), the effect of porosity level can also be notified. Approximately in the region 1.5 to 2.5 nm the slope of figure for the optical absorption coefficient is large for large porosity level but its slope is small after this region when compared to the figure with low porosity level and our results are in conformity with other observations.

### **4.3 Dependence of imaginary part of the dielectric function on porosity level of nanoporous silicon quantum dot**

With the help of eq. (4.6) and eq. (4.2-4.4) a parallel effect is also found for the imaginary part of the dielectric function as that of absorption coefficient. The plot of imaginary part of the dielectric function verses effective size (1-10 nm) for clean, hydrogen and oxygen passivated porous silicon nanoclusters at a given porosity level,  $n=1.32$  and photon energy (3eV) is shown in fig.4.5 and when we change only the porosity level to the value 1.42, the plot is shown in fig.4.6.

As in the case of absorption coefficient, Imaginary part of the dielectric function also strongly depends on the size of nanoparticles. In the very small size (~1.5-2.5 nm) the effects of surface passivation and quantum confinement are strongly dominant due the reasons mentioned under the section 4.2. As we can see from figs.4.5 and 4.6, in this region imaginary part of the dielectric function increases with increasing size of nanoparticles but as we continuo to increase the size of nanoparticles imaginary part of the dielectric function decreases. This is because for large size both surface and quantum confinement effects play very little role on imaginary part of the dielectric function. When we compare figures 4.5 and 4.6, the effect of porosity level can also be understood. Approximately in the region 1.5 to 2.5 nm the slope of figure for the imaginary part of the dielectric function is large for large porosity level but its slope is small after this region when compared to the figure with low porosity level. Turning point of the figure

with higher porosity level takes place before the figure with lower porosity level. This point also works for the absorption coefficient figures.

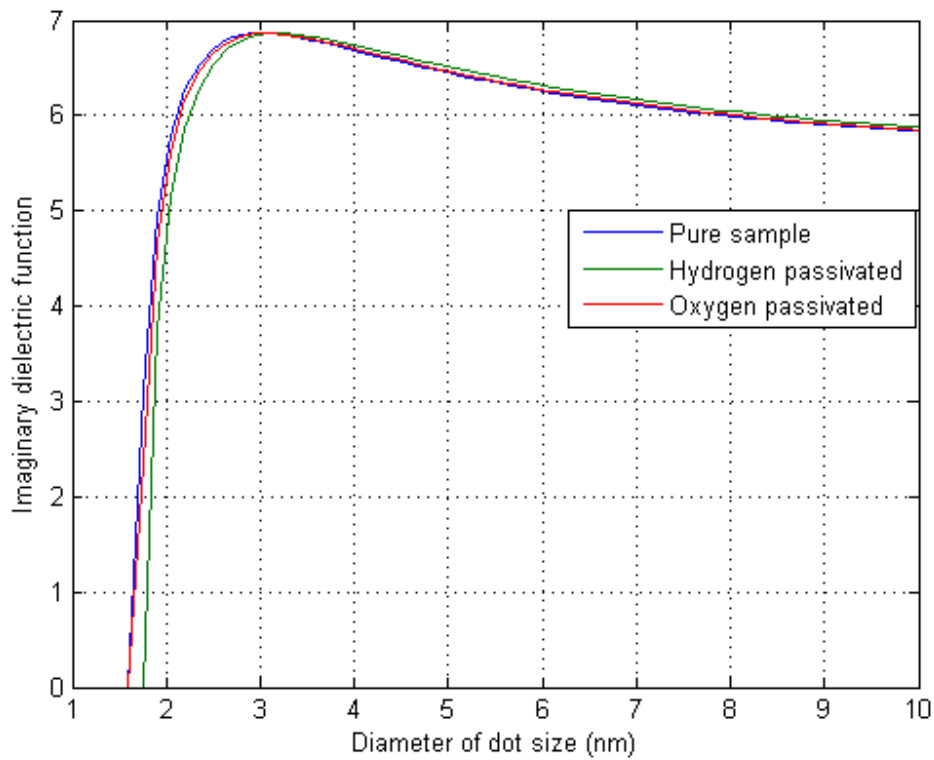


Figure.4.5. Imaginary part of dielectric function as a function of porous silicon nanocluster (quantum dot) size at a given photon energy  $\hbar\omega=3\text{eV}$ . For both pure and passivated samples  $\alpha = 1.32$  (10% to 20% porosity).

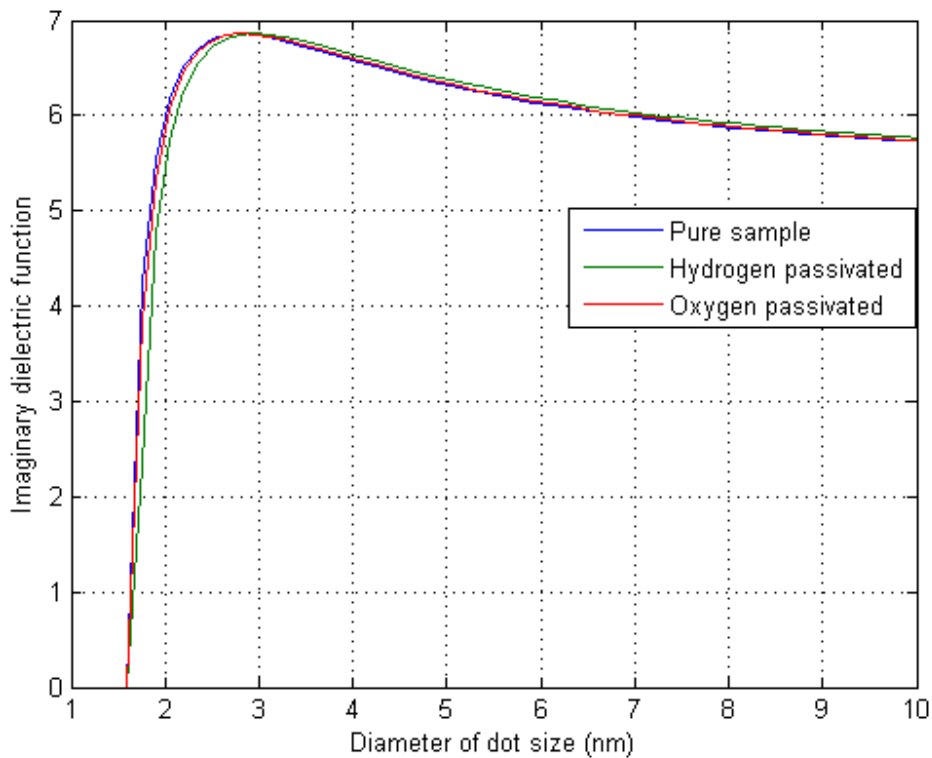


Figure.4.6. Imaginary part of dielectric function as a function of porous silicon nanocluster (quantum dot) size at a given photon energy  $\hbar\omega=3\text{eV}$ . For both pure and passivated samples  $\alpha = 1.42$  (30% to 40% porosity).

#### 4.4 Dependence of Oscillator strength on porosity level of nanoporous silicon quantum dot

Finally using eq.(4.7) and eq.(4.2-4.4) the plot of the oscillatory strength versus effective size (1-10nm) for clean, hydrogen and oxygen passivated nanoporous silicon quantum dot at a given photon energy (3eV) and porosity level,  $\alpha=1.32$  is shown in fig.4.7 and when we change only the porosity level to the value 1.42, the plot is shown in fig.4.7.

Here we found that oscillator strength increases as the size of nanoparticles decreases and we also observed that the oscillator strength increases on passivating the surface of the cluster with oxygen and hydrogen respectively. So the oscillator strength of nanoporous silicon quantum dot strongly depends both

on the size of the nanoparticles (on quantum confinement), and on the surface passivation (surface effect). Furthermore, we also found that oscillator strength decreases as the porosity level increases (compare figs.4.7 and 4.8 with each other).

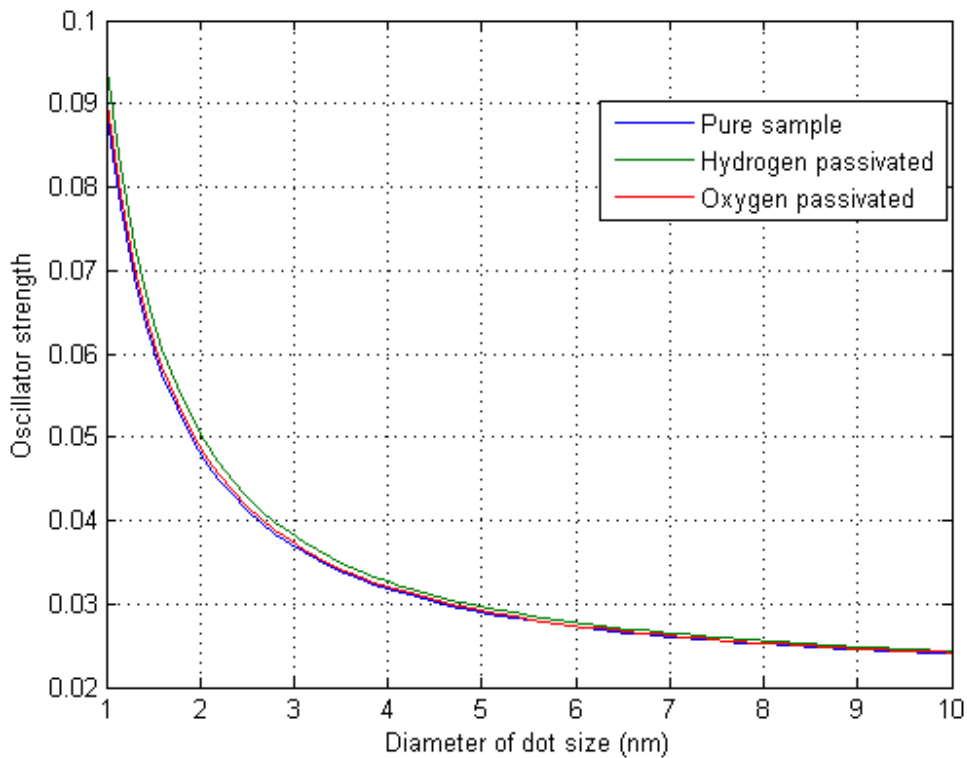


Figure.4.7.Oscillator strength as a function of porous silicon nanocluster (quantum dot) size at a given photon energy  $\hbar\omega=3\text{eV}$ . For both pure and passivated samples  $\alpha=1.32$  (10% to 20% porosity).

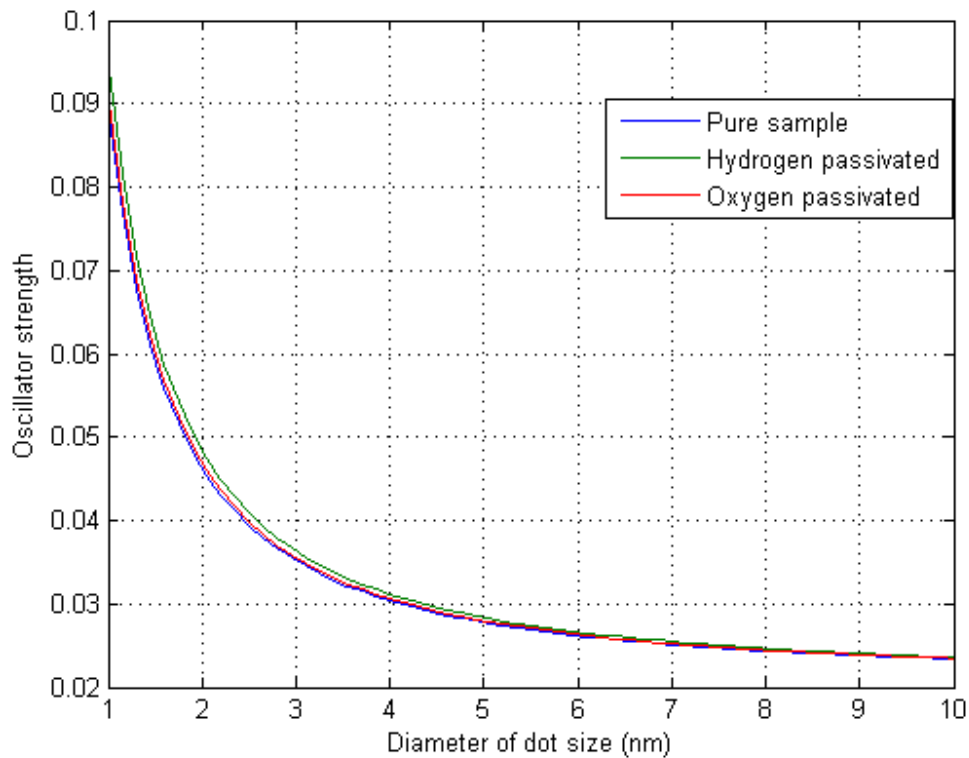


Figure.4.8.Oscillator strength as a function of porous silicon nanocluster (quantum dot) size at a given photon energy  $\hbar\omega=3\text{eV}$ . For both pure and passivated samples  $\alpha =1.42$  (30% to 40% porosity).

## 4.5 Factors that affect peak of photoluminescence

To conclude our results of discussions, now we consider eq. (3.4.7) and the plot of the normalized PL intensity verses effective size (1-6nm) at the given values of  $\gamma =1.32$  and 1.42 are shown in figures 4.9 and 4.10 respectively. In these two figures we want to observe the effect when the porosity level changes. As we can see from the two figures the effect of porosity level on the photoluminescence peak shifts towards left or to the smaller wavelength of visible spectrum (blue shifted) is not so much pronounced. The plot of the normalized PL intensity verses effective size (1-6nm) at the given value of  $\gamma =1.32$  and for values of mean size of nanoporous silicon quantum dots which are different from mean sizes of the same material indicated in figures 4.9 and 4.10 is shown in figure .4.11. Here we want to see the effect of mean size of quantum dots on photoluminescence peak shifts.

When we looked at the figures below, we realized that the photoluminescence peak shifts towards left or to the smaller wavelength of visible spectrum (blue shifted) as the dots size decreases, which is expected. We found that width of size distribution and the average size of quantum dots are the main factors that cause such shifts and our results are in conformity with different experimental and theoretical results.

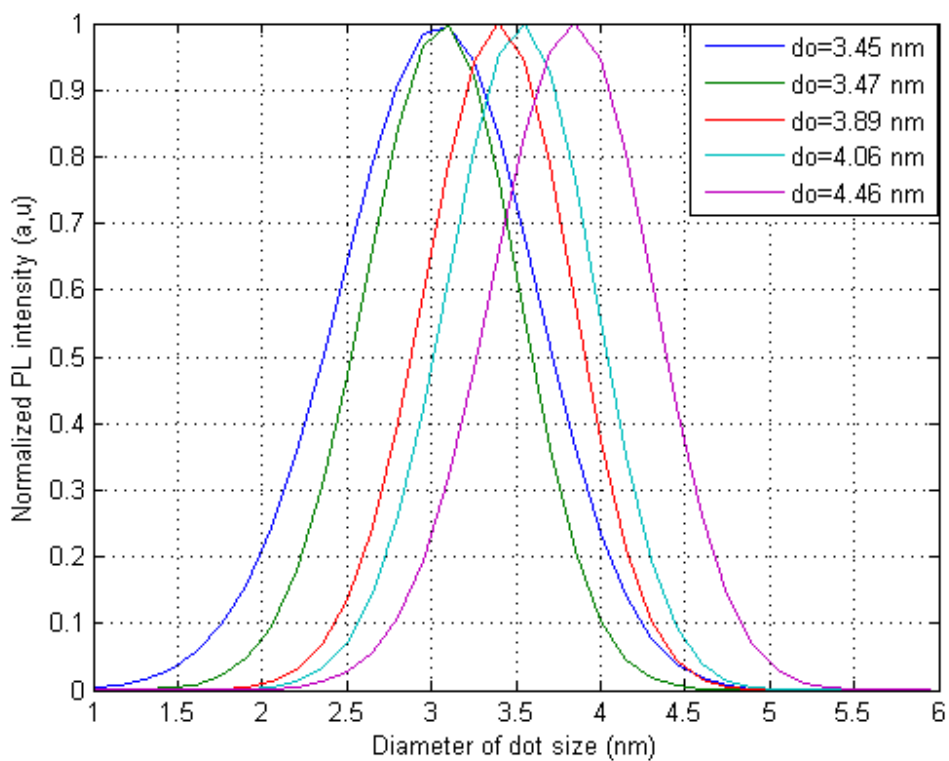


Figure.4.9. Normalized PL intensity versus size of nanoporous silicon cluster (quantum dot) for  $\gamma = 1.32$  (10% to 20% porosity).

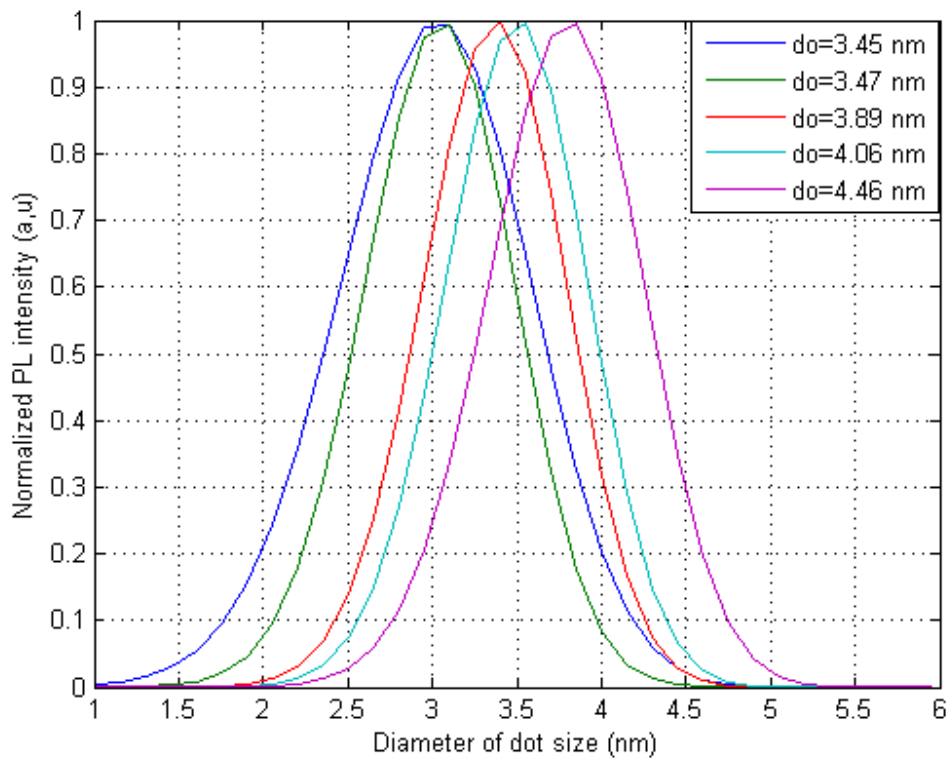


Figure.4.10. Normalized PL intensity versus size of nanoporous silicon cluster (quantum dot) for  $\gamma = 1.42$  (30% to 40% porosity).

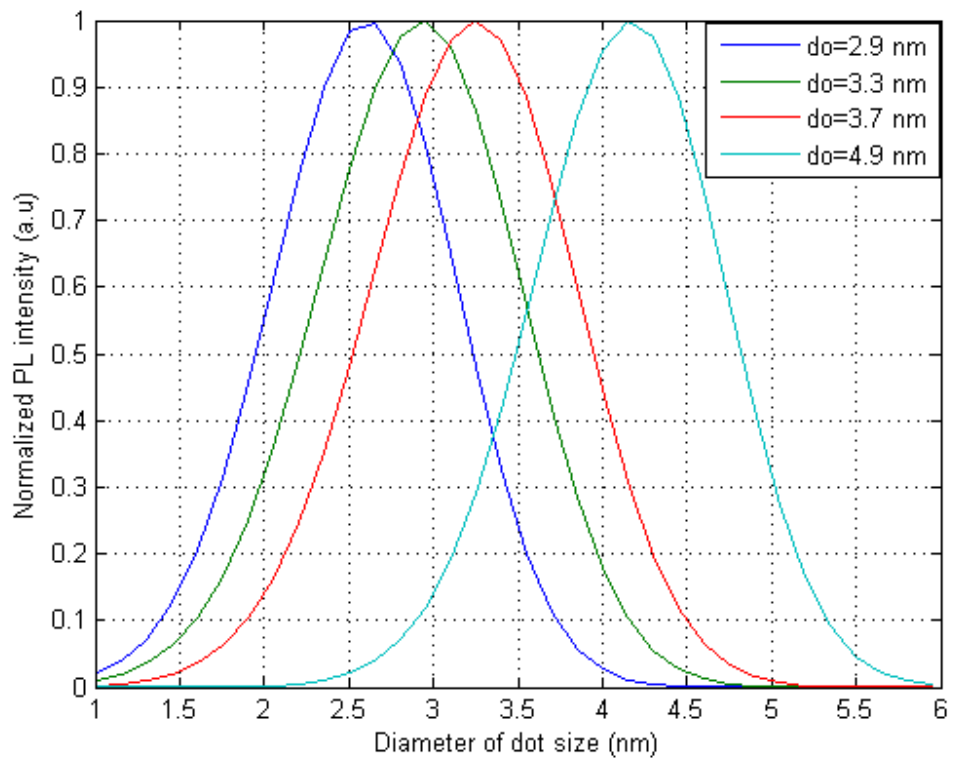


Figure.4.11. Normalized PL intensity versus size of nanoporous silicon cluster (quantum dot) for  $\gamma = 1.32$  (10% to 20% porosity).

## Chapter Five

### Conclusions and future outlook

In this thesis our main aim was to investigate mechanism of light emission from porous silicon nanocluster (quantum dot) and to calculate analytically the optical properties of this material. In order to characterize the optical properties, the density of states which depend on the dimensionality of the system is necessary. With the help of joint density of states and momentum matrix elements we derive the expressions for optical absorption coefficient, dielectric function and oscillator strength. These optical parameters are implicit function of nanoporous silicon quantum dot diameter through energy gap. We found that energy gap of nanoporous silicon quantum dot depends not only on the size or diameter of the dot (quantum confinement effect) but also on surface passivation (surface effect) and porosity level. After explaining the dependence of band gap as a function of effective nanocluster size (quantum dot), we found out the variation of optical absorption coefficient, oscillator strength and imaginary part of dielectric function with dot size porous silicon and porosity level for silicon nanoclusters of clean, hydrogen and oxygen passivated samples obtained from the joint density of states, confinement and surface effects of silicon nanoclusters. We have also noted that, in addition to quantum confinement, surface passivation and porosity level, temperature is also a critical parameter which affects the optical properties of porous silicon.

Our ultimate interest was to observe size, surface passivation and porosity level dependent of energy gap, optical absorption coefficient, oscillator strength and dielectric function. The energy gap of silicon nanoporous quantum dot increases as its size decreases. In addition, the variation of energy gap was also observed by varying porosity level and we found that energy gap decreases with increasing the value of  $\alpha$  and it increases with increasing value of  $c$ . The dependence of absorption coefficient on size, surface passivation and porosity level is observed in a similar way as that of dielectric constant. In the very small size ( $\sim 1.5-2.5$  nm) both absorption coefficient and dielectric constant increase rapidly with increasing size because in this very small region the effects of surface passivation and quantum confinement are strongly dominant for the reason that at very small size large volume fraction of the near surface region over the crystalline core (surface effect) and position of carriers is largely confined (quantum confinement effect). Approximately in the region 1.5 to 2.5 nm the slope of figures for the optical absorption coefficient and dielectric constant is large for large porosity level but its slope is small after this region when compared to

the figure with low porosity level. Moreover, in this very small region the effect of passivating the surface of the cluster with oxygen has greater effect on these optical parameters than passivating the surface of the cluster with hydrogen but after this small region the effect of hydrogen takeover the effect of oxygen and our results are in conformity with experimental findings. We also observed that oscillator strength increases as the size of nanoparticles decreases and it increases on passivating the surface of the cluster with oxygen and hydrogen respectively. Furthermore, we also found that oscillator strength decreases as the porosity level increases and the agreement between our results and the experimental findings is not bad.

From the expression we obtained for PL intensity, we found that width of size distribution and the average size of quantum dots are the main factors that cause the photoluminescence peak shifts towards left or to the smaller wavelength of visible spectrum (blue shifted) and our results are in conformity with other experimental and theoretical results.

Bulk silicon has a problem for light emitting applications due to its indirect band gap and short non-radiative lifetime, while nanostructuring of Si comprises porous silicon, quantum dots, quantum wells and nanoclusters that can exhibit strong photoluminescence at room temperature which is observed only after a drastic reduction of silicon size and this has been related to quantum confinement effect and surface passivation that alters indirect band gap to direct band gap. Although quantum confinement alone cannot explain the whole physics of silicon nanostructures but gives explanation for the observation of luminescence. In case of porous silicon the varying porosity along with crystallites size play role in deciding PL.

Silicon nanostructures have tremendous applications in the photoluminescence, optoelectronic and photonic devices. They can be easily integrated into silicon wafer processing and utilized for biological, chemical, optical sensors and memory devices. It has been discussed that porous silicon can be fabricated by electrochemical anodization of bulk silicon in an HF electrolyte.

The study of silicon nanostructures with their optical properties is still in infant stage. In particular, obtaining light, especially the visible part, is one of the top findings in the present days and still it is a field of active research area. For instance, the role of bond distribution, impurities, phonons, excitons, and relaxational mechanisms are some of the open questions that has to be addressed for accurate quantification of visible PL.

# Appendices

**A:** A MATLAB program to plot optical band gap Vs dot size taking porosity parameters into account

i)  $d=1:0.15:10;$

$c_1=4.5, \alpha_1=1.32, \alpha_2=1.42;$

$eg1=1.12+4.5./ (d.^{1.32});$

$eg2=1.12+4.5./ (d.^{1.42});$

Plot (d, eg1, d, eg2)

Legend ('c1=4.5;  $\alpha_1=1.32$ ', 'c1=4.5;  $\alpha_2=1.42$ ')

xlabel ('Diameter of dot size (nm)'), ylabel ('Energy gap (eV)')

ii)  $d=1:0.15:10;$

$c_2=6.2, \alpha_1=1.32, \alpha_2=1.42;$

$eg3=1.12+6.2./ (d.^{1.32});$

$eg4=1.12+6.2./ (d.^{1.42});$

Plot (d, eg3, d, eg4)

Legend ('c1=6.2;  $\alpha_1=1.32$ ', 'c2=6.2;  $\alpha_2=1.42$ ')

xlabel ('Diameter of dot size (nm)'), ylabel ('Energy gap (eV)')

**B:** A MATLAB program to plot Absorption coefficient Vs dot size taking surface passivation and porosity level into account.

i)  $d=1:0.15:10;$

Pure sample=3.73;

Hydrogen passivated=4.042;

Oxygen passivated=3.82;

$eg1=1.12+3.73./ (d.^{1.32});$

$eg2=1.12+4.042./ (d.^{1.32});$

```

eg3=1.12+3.82./ (d. ^1.32);
ac1=5.15e5.*eg1.*((eg1+0.044). / (3*eg1+0.088)).*sqrt (3-eg1);
ac2=5.15e5.*eg2.*((eg2+0.044). / (3*eg2+0.088)).*sqrt (3-eg2);
ac3=5.15e5.*eg3.*((eg3+0.044). / (3*eg3+0.088)).*sqrt (3-eg3);
Plot (d, ac1, d, ac2, d, ac3);
Legend ('pure sample', 'Hydrogen passivated', 'Oxygen passivated')
xlabel ('Diameter of dot size (nm)'), ylabel ('Absorption coefficient (1/ cm)')
ii) d=1:0.15:10;

```

```

Pure sample=3.73;
Hydrogen passivated=4.042;
Oxygen passivated=3.82;
eg1=1.12+3.73./ (d. ^1.42);
eg2=1.12+4.042./ (d. ^1.42);
eg3=1.12+3.82./ (d. ^1.42);
ac1=5.15e5.*eg1.*((eg1+0.044). / (3*eg1+0.088)).*sqrt (3-eg1);
ac2=5.15e5.*eg2.*((eg2+0.044). / (3*eg2+0.088)).*sqrt (3-eg2);
ac3=5.15e5.*eg3.*((eg3+0.044). / (3*eg3+0.088)).*sqrt (3-eg3);
Plot (d, ac1, d, ac2, d, ac3);
Legend ('pure sample', 'Hydrogen passivated', 'Oxygen passivated')
xlabel ('Diameter of dot size (nm)'), ylabel ('Absorption coefficient (1/ cm)')

```

**C:** A MATLAB program to plot imaginary part of dielectric function Vs dot size by considering surface passivation and porosity level.

```

i) d=1:0.15:10;
Pure sample=3.73;
Hydrogen passivated=4.042;
Oxygen passivated=3.82;
eg1=1.12+3.73./ (d. ^1.32);
eg2=1.12+4.042./ (d. ^1.32);

```

```

eg3=1.12+3.82./ (d. ^1.32);
ε1=10.22.*eg1.*((eg1+0.044). /(3*eg1+0.088)).*sqrt(3-eg1);
ε2=10.22.*eg2.*((eg2+0.044). /(3*eg2+0.088)).*sqrt(3-eg2);
ε3=10.22.*eg3.*((eg3+0.044). /(3*eg3+0.088)).*sqrt(3-eg3);
Plot (d, ε1, d, ε2, d, ε3);
Legend ('pure sample', 'Hydrogen passivated', 'Oxygen passivated')
xlabel ('Diameter of dot size (nm)'), ylabel ( 'Imaginary dielectric function ')

```

ii) d=1:0.15:10;

```

Pure sample=3.73;
Hydrogen passivated=4.042;
Oxygen passivated=3.82;
eg1=1.12+3.73./ (d. ^1.42);
eg2=1.12+4.042./ (d. ^1.42);
eg3=1.12+3.82./ (d. ^1.42);
ε1=10.22.*eg1.*((eg1+0.044). /(3*eg1+0.088)).*sqrt(3-eg1);
ε2=10.22.*eg2.*((eg2+0.044). /(3*eg2+0.088)).*sqrt(3-eg2);
ε3=10.22.*eg3.*((eg3+0.044). /(3*eg3+0.088)).*sqrt(3-eg3);
Plot (d, ε1, d, ε2, d, ε3);
Legend ('pure sample', 'Hydrogen passivated', 'Oxygen passivated')
xlabel ('Diameter of dot size (nm)'), ylabel ( 'Imaginary dielectric function ')

```

**D:** A MATLAB program to plot oscillator strength Vs dot size taking surface passivation and porosity level into account.

```

i) d=1:0.15:10;
Pure sample=3.73;
Hydrogen passivated=4.042;
Oxygen passivated=3.82;
eg1=1.12+3.73./ (d. ^1.32);
eg2=1.12+4.042 (d. ^1.32);

```

```

eg3=1.12+3.82./ (d. ^1.32);
f1=5.5e-2.*((eg1+0.044)./(3*eg1+0.088)).*eg1;
f2=5.5e-2.*((eg2+0.044)./(3*eg2+0.088)).*eg2;
f3=5.5e-2.*((eg3+0.044)./(3*eg3+0.088)).*eg3;
Plot (d, f1, d, f2, d, f3);
Legend ('pure sample', 'Hydrogen passivated', 'Oxygen passivated')
xlabel ('Diameter of dot size (nm)'), ylabel ('Oscillator strength ')
ii) d=1:0.15:10;

```

```

Pure sample=3.73;
Hydrogen passivated=4.042;
Oxygen passivated=3.82;
eg1=1.12+3.73./ (d. ^1.42);
eg2=1.12+4.042 (d. ^1.42);
eg3=1.12+3.82./ (d. ^1.42);
f1=5.5e-2.*((eg1+0.044)./(3*eg1+0.088)).*eg1;
f2=5.5e-2.*((eg2+0.044)./(3*eg2+0.088)).*eg2;
f3=5.5e-2.*((eg3+0.044)./(3*eg3+0.088)).*eg3;
Plot (d, f1, d, f2, d, f3);
Legend ('pure sample', 'Hydrogen passivated', 'Oxygen passivated')
xlabel ('Diameter of dot size (nm)'), ylabel ('Oscillator strength ')

```

**E:** A MATLAB program to plot normalized photoluminescence intensity Vs dot size taking porosity level into account.

```

i) d=1:0.15:6;
de=3.73./ (d. ^1.32)-0.11./ (d. /2)-0.055679;
ia=exp (-(((3.73./de).^0.7576-3.45).^2)/1.03);
ib=exp (-(((3.73./de).^0.7576-3.47).^2)/0.64);
ic=exp (-(((3.73./de).^0.7576-3.89).^2)/0.62);
id=exp (-(((3.73./de).^0.7576-4.06).^2)/0.63);

```

```

ie=exp (-(((3.73./de).^0.7576-4.46).^2)/0.79);
plot(d,ia,d,ib,d,ic,d,id,d,ie)
Legend ('do=3.45 nm',' do=3.47 nm','do=3.89 nm','do=4.06nm',do=4.46 nm')
xlabel ('Diameter of dot size (nm)'), ylabel ('Normalized PL intensity (a .u) ')
ii) d=1:0.15:6;
de=3.73./ (d. ^1.42)-0.11./ (d. /2)-0.055679;
ia=exp (-(((3.73./de).^0.7042-3.45).^2)/1.03);
ib=exp (-(((3.73./de).^0.7042-3.47).^2)/0.64);
ic=exp (-(((3.73./de).^0.7042-3.89).^2)/0.62);
id=exp (-(((3.73./de).^0.7042-4.06).^2)/0.63);
ie=exp (-(((3.73./de).^0.7042-4.46).^2)/0.79);
plot(d,ia,d,ib,d,ic,d,id,d,ie)
Legend ('do=3.45 nm',' do=3.47 nm','do=3.89 nm','do=4.06nm',do=4.46 nm')
xlabel ('Diameter of dot size (nm)'), ylabel ('Normalized PL intensity (a .u) ')
iii) d=1:0.15:6;
de=3.73./ (d. ^1.32)-0.11./ (d. /2)-0.055679;
ia=exp (-(((3.73./de).^0.7576-2.9).^2)/0.87);
ib=exp (-(((3.73./de).^0.7576-3.3).^2)/1.09);
ic=exp (-(((3.73./de).^0.7576-3.7).^2)/1.17);
id=exp (-(((3.73./de).^0.7576-4.9).^2)/1.17);
plot(d,ia,d,ib,d,ic,d,id )
Legend ('do=2.9 nm',' do=3.3 nm','do=3.7 nm','do=4.9 nm')
xlabel ('Diameter of dot size (nm)'), ylabel ('Normalized PL intensity (a .u) ')

```

# Bibliography

- [1] W. K.ChoiThio, H. H. THIO, S. P.Ng, V. Ng and B. A. Cheong, Philosophical Magazine B, **80**, No. 4, 739 (2000)
- [2] M.Fujii, A.polman in silicon based photonics, App. phy let.711198 (1997)
- [3] H. Nalwa, Nanostructured Materials and Nanotechnology, **4** Academic Press (2000).
- [4] P. D. J. Calcott, K. J. Nash, L. T. Canham, M. J.Kane and D.Brumhead, J.Phys. **81**, (1993)
- [5] K. E .Andersen, C. Y .Fong and W. E .Pickett, J. Nano. Crys. Solids. **64** (2000).
- [6] [http:// WWW.ct.infn.it/matis](http://WWW.ct.infn.it/matis) (Accessed in March 2010).
- [7] A. P. Alivisatos, J. Phys. Chem. **100**, 13226 (1996).
- [8] P. Bettotti, M. Cazzanelli, L. Dal Negro, B. Danese, Z. Gaburro, C. J. Oton, G.Vijaya Prakash and L. Pavesi, J. Phys,.: Condensed Matter **14**, 8253 (2002). .
- [9] Nanoscience and nanotechnologies, The Royal Society & The Royal Academy of Engineering, Latimer Trend Ltd, Plymouth, UK (2004)
- [10] X. Badel in Electrochemically etched pore arrays in silicon for X-ray imaging detectors, Ph.D. thesis, KTH, Stockholm, Sweden, (2005)
- [11] A. G. Cullis, L. T. Canham, and P. D. J. Calcott, J. Appl. Phys., **82**, 909 (1997)
- [12] Nagendra, N.Beladakere, VISIONGLOW IP PTY LTD: 8/2523014 United States

Patent 6730282,(2004)

- [13] Lorenzo, Pier Paolo, Fulvio: 09/985642 United States Patent 6730282,(2004)
- [14] M. L. Ciurea, I.Stavarache and V. Iancu, J. Nano. Crys. Solids. **15**, 1802 (2004).
- [15] [http:// WWW.nanohub.org/nanomaterials](http://WWW.nanohub.org/nanomaterials) (Accessed in March 2010).
- [16] M . V .Wolkin, J . Jorne, PM . Fauchet, G . Allan and C . Delerue. Phys. Lett. **83**,(1999).
- [17] P.C .Searson, J. M. Maculay and F. M. Ross, J. Appl. Phys. **72**, (1992).
- [18] S. L. Zang, S. P. Wong, I. H. Wilson, S. K. Hardk, Z. F. Liu and S.M. Cai. Appl. Phys. Lett. **69**, (1996).
- [19] K. D. Hirschman, L. Tsybeskov, S. P. Duttagupta and F. M. Fauchet. Nature **384**, (2004).
- [20] V. Kumar and Y. Kawazoe, Phys. Rev. Lett. **87**, 045503 (2001).
- [21] L. Pavesi, L. D. Negro, C. Mazzoleni, G. Franzo and F. Priolo, Nature. **408**, 440 (2000).
- [22] L. Pavesi and R. Guardini, Brazilian J. Phys. **26**, No.172 (1996).
- [23] S. K. Ghoshal, Devendara Mohan, Tadesse Tenaw Kassa and Sunita Sharma, International Journal of Modern Physics B, **21**, No. 22 3783 (2007).
- [24] J.C.Vial, A.Bsiesy, F.Gaspard, R.Herino, M.Ligeon, F.Muller, and R.Romestain, Physical Rev.B, **45**, No.24 (1992).
- [25] L. C. Lenchyshyn, M. L. W. Thewalt, J. C. Sturm, et al., High quantum efficiency Photoluminescence from localized excitons in Si<sub>1-x</sub>Gex, Applied Physics Letters, **60**, no. 25, pp.31743176, (1992)
- [26] Long Yongfu, Ge Jin, Ding Xunmin and Hou Liaoyuan, Journal of semiconductors, **30**, No.6 (2009)
- [27] Shuji Hasegawa, Surface state bands on silicon as electron systems in reduced dimensions at atomic scales. J. Phys.: Condensed Matter **12**, pp. R463 - R495 (2000).

- [28] M. V. Wolkin, J. Jorne and P.M. Fauchet, *Phys. Rev. Lett.*, **82**, 1 (1999).
- [29] Zhiyong Zhou, Michael L. Steigerwald, Richard A. Friesner, Louis Brus and Mark S. Hybertsen, *Phys. Rev. B*, **71**, 245308 (2005).
- [30] Klaus Sattler, Department of Physics and Astronomy, University of Hawaii, Honolulu, Hawaii, USA, **5**, P.73, (2002)
- [31] B.P. Singh, *Bull. Mater. Sci.* **29**, No. 6, pp. 559 (2006).
- [32] V. Ranjan and Vijay A. Singh, *Phys. Rev. B*, **58**, 3 (1998).
- [33] J.P. Proot, C. Delerue and G. Allan, *Appl. Phys. Lett.* **61**, 16 (1992)
- [34] Tripathy, R. K. Soni, S. K. Ghoshal and K. P. Jain, *Bull. Mater. Sci.* **24**, No. 3, pp. 285-289, (2001).

## Declaration

I, the undersigned, declare that this thesis work is my original work, has not been presented for a degree in this or other universities, and all sources of materials used for the thesis work have been fully acknowledged.

Name:Adem Beriso

Signature:.....

This thesis has been submitted for examination with my approval as a university advisor.

Name:Dr.Sib Krishna Ghoshal

Signature:.....

Addis Ababa University

Department of physics

June, 2010

# Acknowledgements

First and for most, I would like to praise the name of the Almighty God (Allah), for giving me health, patience, courage and protection to complete this work; without whom nothing is possible.

Very special thanks to my instructor and advisor, Dr. Sib Krishna Ghoshal for his many suggestions and constant support during the course of this thesis. Especially, his limitless and invaluable effort in guiding, advising, supervising, encouraging, understanding my exceptional problem, educating me in this field and providing the necessary materials for the accomplishment of this thesis gives me a great pleasure.

Words cannot express the gratitude I have for all the support and love of my wife, Hayat Edo over the years.

Many thanks to Mr. Fayisa Dabo for all what he has done for me as a brother and friendship is beyond words to express. Thank you so much and I would like to say congratulation for the successful completion of your study.

Finally, I wish to thank the following: Seid Mohammed, Seyfan kelil, Abera Abebe, Makida Edo, Tahir Midakso, Isaac Haile and Berhanu Daba -thank you for your remarkable support and motivation.

Addis Ababa, Ethiopia  
June, 2010

Adem Beriso

